Check for updates

Received: 14 October 2025 | Revised: 3 March 2026 | Accepted: 21 March 2026

DOI: 10.1111/bph.70457

RESEARCH ARTICLE

5-HT_{2A} receptor agonism by *tert*-leucinamide and valinamide synthetic cannabinoids: In vitro and in vivo evidence

Giorgia Corli[1] | Deborah Rudin[2,3] | Dino Luethi[2,3] | Matthias E. Liechti[2,3] | Sabrine Bilel[1] | Matteo Marti[1,4] | Henrik Green[5,6,7] | Manuela Carla Monti[5] | Caitlyn Norman[5]

[1]Department of Excellence of Translational Medicine, Section of Legal Medicine, LTTA Center and University Center of Gender Medicine, University of Ferrara, Ferrara, Italy

[2]Division of Clinical Pharmacology and Toxicology, Department of Pharmaceutical Sciences, University of Basel, Basel, Switzerland

[3]Division of Clinical Pharmacology and Toxicology, Department of Biomedicine, University Hospital Basel, Basel, Switzerland

[4]Department of Anti-Drug Policies and Other Addictions, Presidency of the Council of Ministers, Collaborative Center for the Italian National Early Warning System, NEWSD, Rome, Italy

[5]Department of Biomedical and Clinical Science, Division of Clinical Chemistry and Pharmacology, Linköping University, Linköping, Sweden

[6]Department of Forensic Genetics and Forensic Toxicology, National Board of Forensic Medicine, Linköping, Sweden

[7]Department of Biomedical and Clinical Science, Science for Life Laboratory, Linköping University, Linköping, Sweden

Correspondence
Manuela Carla Monti and Caitlyn Norman, Department of Biomedical and Clinical Science, Division of Clinical Chemistry and Pharmacology, Linköping University, Linköping, Sweden.
Email: manuela.monti@unibas.ch and caitlyn.norman@liu.se

Funding information
University of Ferrara, Grant/Award Numbers: FAR 2024, FAR 2025; Anti-Drug Policies Department, Presidency of the Council of

Abstract

Background and Purpose: New synthetic cannabinoid receptor agonists (SCRAs) are associated with severe adverse effects, including unexpected psychiatric symptoms. These compounds are mainly active through their potent agonism on the cannabinoid receptors CB_1 and CB_2. Recently, evidence of the direct interaction of some SCRAs with the serotonergic 5-HT receptors has emerged.

Experimental Approach: SCRAs were screened for in vitro 5-HT_{2A} receptor activity using AequoScreen® intracellular Ca^{2+} release and inositol monophosphate (IP_1) formation assays. The pharmaco-toxicological effects induced by the administration of the most effective compound in vitro (AB-5′F-BUTINACA) were investigated in male CD-1 mice with specific focus on its interaction with CB_1 and 5-HT_{2A} receptors.

Key Results: Many SCRAs with a valinamide (AB) or *tert*-leucinamide (ADB) head moiety had in vitro activity at the 5-HT_{2A} receptor at high concentrations with AB-5′F-BUTINACA and ADB-BUTINACA amongst the most efficacious. In vivo studies showed that AB-5′F-BUTINACA caused neurological changes, sensorimotor alteration, antinociception, hypothermia, reduction in breath rate and hypolocomotion in mice. The neurological, sensorimotor, and thermal antinociceptive effects were mediated by CB_1 and 5-HT_{2A} receptors, as they were prevented by pretreatment with the selective CB_1 and 5-HT_{2A} receptor antagonists (NESS0327 and MDL100907, respectively).

Conclusion and Implications: This study demonstrated for the first time that SCRAs with a valinamide or *tert*-leucinamide head moiety activate the 5-HT_{2A} receptor. Agonism of the compound AB-5′F-BUTINACA at the 5-HT_{2A} receptors resulted in in vivo effects. Our data revealed potential risks related to SCRA consumption that could exacerbate unexpected psychiatric conditions.

KEYWORDS

5-HT_{2A} receptor, ADB-BUTINACA, mice, new psychoactive substances, potency, synthetic cannabinoid receptor agonists

Manuela Carla Monti and Caitlyn Norman contributed equally.

This is an open access article under the terms of the Creative Commons Attribution License, which permits use, distribution and reproduction in any medium, provided the original work is properly cited.
© 2026 The Author(s). *British Journal of Pharmacology* published by John Wiley & Sons Ltd on behalf of British Pharmacological Society.

Ministers, Italy; Svenska Sällskapet för Medicinsk Forskning (Swedish Society for Medical Research, SSMF), Grant/Award Number: PG-24-0356-H-01; the Swiss National Science Foundation (SNSF), Grant/Award Number: 217677; VINNOVA (Sweden's Innovation Agency), Grant/Award Number: 2019-03566; European Union's Horizon 2020 research and innovation program; Eurostars-3 Joint Programme, Grant/Award Number: E!2297; Strategic Research Area in Forensic Sciences

1 | INTRODUCTION

Synthetic cannabinoid receptor agonists (SCRAs) are a structurally diverse class of new psychoactive substances (NPS) that are sold as recreational drugs on unregulated markets. SCRAs mimic the intoxicating effects of the main psychoactive component of cannabis, **Δ^9-tetrahydrocannabinol** (Δ^9-THC), by acting at the same primary target, the **cannabinoid 1 (CB1) receptor**. However, SCRAs are often significantly more potent and efficacious than Δ^9-THC at CB_1 receptors and produce severe adverse effects, some of which more closely resemble those of psychostimulants than those of cannabis (Darke et al., 2021). In particular, increasing evidence suggests that mechanisms underlying some adverse effects induced by SCRAs, including anxiety and psychotic symptoms, are mediated by the complex and not well understood interplay of the CB_1 receptor and endocannabinoid system with the dopaminergic and serotonergic systems (Fantegrossi et al., 2018; Ibarra-Lecue et al., 2018, 2021; Ossato et al., 2017). Published data has already highlighted the potential of SCRAs to modulate the synthesis (Nakazi et al., 2000), release (Moranta et al., 2004) and uptake (Steffens & Feuerstein, 2004) of **5-HT** in different areas of the rodent brain.

Receptors for 5-HT are primarily located in pyramidal cells of the prefrontal cortex (PFC) and regulate various functions, including mood and impulse control. The serotonergic system is associated with many psychiatric disorders, including depression, schizophrenia, anxiety and addiction, making it one of the most important neurotransmitters for mental health (S. Lin et al., 2014). The endocannabinoid system is involved in many of the same physiological processes (e.g., mood and behaviour) and functional interactions between the serotonergic and endocannabinoid systems have therefore been subject to a broad range of research (Haj-Dahmane & Shen, 2011; Hill et al., 2006; Peters et al., 2021; Salaga et al., 2019). Reported psychotic adverse effects of SCRAs have sparked interest in potential non-cannabinoid receptor involvement, with particular interest in **5-HT_{2A}** receptors, the primary target of psychedelics, such as **psilocin** and **lysergic acid diethylamide** (LSD) (Ibarra-Lecue et al., 2021). Although Δ^9-THC does not have affinity for the 5-HT receptors, some SCRAs, such as **JWH-018**, **AM-2201** or 5F-PB-22. might interact with a number of 5-HT receptors, including **5-HT_{1A}**, 5-HT_{2A} and **5-HT_{2B}** receptors (Corli, Tirri, et al., 2024; Wiley et al., 2016; Yano et al., 2020). This suggests that interaction with the 5-HT receptors may contribute to the greater adverse psychiatric effects of SCRAs, compared to those of Δ^9-THC.

What is already known?

- Strong psychoactive (e.g., pro-psychotic) effects are observed for synthetic cannabinoid receptor agonists (SCRAs).
- CB_1 mediation of the serotonergic system is a mechanism for some effects of SCRAs.

What does this study add?

- Many valinamide (AB) and *tert*-leucinamide (ADB) SCRAs show in vitro activity at the 5-HT_{2A} receptor.
- AB-5′F-BUTINACA results in 5-HT_{2A} receptor mediated in vivo effects in mice.

What is the clinical significance?

- Interaction with 5-HT2A receptors may underlie some of the psychiatric adverse effects evoked by SCRAs.

In this study, a set of 15 structurally diverse SCRAs was screened for in vitro activity at the 5-HT_{2A} receptor using an AequoScreen® 5-HT_{2A} intracellular Ca^{2+} release assay. Based on these results, valinamide (n = 10) and *tert*-leucinamide (n = 18) SCRAs were screened and those that displayed some activity were examined further. A 5-HT_{2A} radioligand binding assay was also used to screen 23 SCRAs. The structures of all SCRAs examined in this study can be found in Figures S1.1–S1.3. Finally, the in vivo effects of the most efficacious SCRA, **AB-5′F-BUTINACA**, was studied and its interaction with both the selective CB_1 receptor antagonist **NESS0327** and the 5-HT_{2A} receptor antagonist **MDL100907** was evaluated in CD-1 adult male mice. The present pioneering investigation into the pharmacological profile of SCRAs was aimed at clarifying whether the pro-psychotic effects of SCRAs are related to in vitro activity on serotoninergic receptors, establishing the first evidence of a correlation.

14765381, 2026, 16, Downloaded from https://bpspubs.onlinelibrary.wiley.com/doi/10.1111/bph.70457 by Universita Di Ferrara, Wiley Online Library on [20/10/2026]. See the Terms and Conditions (https://onlinelibrary.wiley.com/terms-and-conditions) on Wiley Online Library for rules of use; OA articles are governed by the applicable Creative Commons License

2 | METHODS

2.1 | AequoScreen® 5-HT$_{2A}$ and CB$_1$ intracellular Ca^{2+} release assay

The AequoZen recombinant Chinese hamster ovary (CHO) K1 cell lines, stably expressing the human 5-HT$_{2A}$ receptor (Revvity, Sollentuna, Sweden; Cat# ES-313-AF; RRID: CVCL_F2AJ) or human CB$_1$ receptor (Revvity, Sollentuna, Sweden; Cat# ES-110-A; RRID: CVCL_F2AK) were used. Advanced DMEM/Ham's F12, DMEM/Ham's F12 without phenol red, 0.25% trypsin–EDTA with phenol red, foetal bovine serum (FBS), geneticin and zeocin were purchased from Thermo Fisher (Gothenburg, Sweden). HEPES buffer, L-glutamine, protease-free bovine serum albumin (BSA), digitonin, adenosine-50-triphosphate disodium salt hydrate (ATP), methanol and dimethyl sulfoxide (DMSO) were procured from Sigma-Aldrich (Stockholm, Sweden). The coelenterazine substrate was from Nanolight Technology (Pinetop, AZ, USA). The structures of all SCRAs examined in this study can be found in Figures S1.1–S1.3.

The apoaequorin system (AequoScreen® assay) is an intracellular calcium (Ca^{2+}) release assay commonly used for measuring G protein coupled receptor (GPCR) activity. Apoaequorin is a protein that in the presence of its substrate coelenterazine converts to the aequorin photoprotein, which has three Ca^{2+} binding sites. Binding of an extracellular ligand to the GPCR leads to the activation of a universal G protein subunit G$_{\alpha16}$, which in turn triggers a series of downstream events, such as the activation of the phospholipase C (PLC) enzyme, that stimulates the release of intracellular Ca^{2+} (Deng et al., 2009). The Ca^{2+} then binds to the aequorin photoprotein, which oxidises the coelenterazine leading to the release of photons that can be measured via a luminescence reader (Wouters et al., 2019).

CHO-K1 cells stably expressing the 5-HT$_{2A}$ receptor, the apoaequorin enzyme, and the Gα_{16} subunit were maintained in a humidified atmosphere at 37°C and 5% CO_2 in Advanced DMEM/Ham's F12 medium supplemented with 10% heat-inactivated FBS, 2.5-μM L-glutamine, 400-μg·ml^{-1} geneticin and 250-μg·ml^{-1} zeocin. CHO-K1 cells stably expressing the CB$_1$ receptor, the apoaequorin enzyme, and the Gα_{16} subunit were maintained in a humidified atmosphere at 37°C and 5% CO_2 in Ham's F12 medium supplemented with 10% heat-inactivated FBS, 400-μg·ml^{-1} geneticin and 250-μg·mL^{-1} zeocin. To perform the assays, cells were trypsinised (10 min, 37°C), centrifuged (200 × *g*, 5 min, room temperature), counted and resuspended at 3 × 10^5 cells·ml^{-1} in DMEM/Ham's F12 without phenol red and supplemented with 15-mM HEPES, L-glutamine and protease-free BSA (0.1%) (further referred to as assay medium). The coelenterazine substrate was added to a final concentration of 2.5 μM and the suspension was incubated for 3 h (room temperature, rotating at 7 RPM·min^{-1}, protected from light). Test solutions were prepared as a 1:3 or 1:8 serial dilution in assay medium with a starting concentration of 70 or 60 μM for the 5-HT$_{2A}$ and CB$_1$ assays, respectively, and then added to white, opaque-welled 96-well plates. For screening, only the top concentration was tested. For the 5-HT$_{2A}$ assay, LSD was included as a reference on each plate, in line with earlier results generated using the AequoScreen® 5-HT$_{2A}$ assay (Åstrand et al., 2020). For the CB$_1$ assay, JWH-018 was included as a reference on each plate, in line with earlier results generated using the AequoScreen® CB$_1$ assay (Åstrand et al., 2020; Green et al., 2025). Digitonin (67 μM) and ATP (6.7 μM) were included on each plate and served as positive controls for coelenterazine loading as both are involved in the non-CB and non-5-HT-dependent release of calcium ions. Blank assay medium was used as a negative control. Using a TECAN Spark 10-M plate reader (Männedorf, Switzerland), 50 μl of the incubated cell suspension was dispensed into each well (approximately 15 × 10^3 cells per well) of the 96-well plate containing the test solutions at reading cycle #10. Luminescence was measured for 25 s (corresponding to 190 additional reading cycles). For each compound, activity was measured in triplicate with different batches of harvested cells.

Absolute luminescence signals were corrected for intra-plate variability in Microsoft Excel 365 using area under the curve (AUC) values and were calculated for each concentration of the test compounds. Values were then blank-corrected by subtracting AUC values of the mean of the blank controls. Data were normalised to the maximum of LSD for 5-HT$_{2A}$ receptors or JWH-018 for CB$_1$ receptors and inter-plate variability was adjusted using the reference values. The normalised values were transferred to GraphPad Prism (Version 10.0.2) to generate concentration-response curves and calculate EC$_{50}$ and E_{max} values by curve fitting via nonlinear regression (three-parameter logistic fit). Results are represented as receptor activity of LSD (%) for 5-HT$_{2A}$ or receptor activity of JWH-018 (%) for CB$_1$ derived from three independent experiments (n = 3), run in triplicate.

2.2 | Inositol monophosphate (IP$_1$) formation assay

5-HT hydrochloride was obtained from Merck (Buchs, Switzerland). AB-5′F-BUTINACA and ADB-5′F-BUTINACA were provided by Linköping University (Section 2.1). ADB-BUTINACA was kindly provided by the Zurich Forensic Science Institute (Zürich, Switzerland). DMSO was purchased from Sigma-Aldrich (Saint Quentin Fallavier, France). Activity testing at the human 5-HT$_{2A}$ receptor relied on the Cisbio IP-One Gq Kit (Cisbio Bioassays SAS, Codolet Cedex, France) that enables the assessment of intracellular IP$_1$ accumulation upon receptor activation, as described before (Arias et al., 2024). In brief, NIH/3 T3 cells stably expressing the human 5-HT$_{2A}$ receptor (RRID: CVCL_F2AP) were seeded at 3000 cells per well into 384-well plates in Opti-MEM medium obtained from Gibco (Thermo Fisher, Zug, Switzerland). Drugs were added to the plates and incubated for 90 min at 37°C and Anti-IP1-Cryptate and IP1-d2 were added and the plate was incubated for an additional 60 min at room temperature. The stimulated formation of IP$_1$ was detected using homogenous time-resolved fluorescence (HTRF) measurements, using a BioTek Synergy H1 Multimode Reader (Agilent Technologies AG, Basel, Switzerland). The obtained data were normalised to the maximal effect of 5-HT, which was measured in parallel. The obtained data (mean ± SEM) were analysed with GraphPad Prism software (Version 10.0.1). Concentration-response curves were fitted via

14765381, 2026, 16, Downloaded from https://bpspubs.onlinelibrary.wiley.com/doi/10.1111/bph.70457 by Universita Di Ferrara, Wiley Online Library on [20/10/2026]. See the Terms and Conditions (https://onlinelibrary.wiley.com/terms-and-conditions) on Wiley Online Library for rules of use; OA articles are governed by the applicable Creative Commons License

non-linear regression (three-parameter logistic fit) to calculate EC_{50} and E_{max} values.

2.3 | In vivo study

2.3.1 | Animals

All animal care and experimental protocols in the present study were in accordance with the UK Animals (Scientific Procedures) Act of 1986 and associated guidelines and the new European Communities Council Directive of September 2010 (2010/63/EU). Experimental protocols were approved by the Italian Ministry of Health (licence no. 223/2021-PR) and by the Animal Welfare Body of the University of Ferrara. Animal studies are reported in compliance with the ARRIVE guidelines (Percie du Sert et al., 2020) and with the recommendations made by British Journal of Pharmacology (Lilley et al., 2020). All possible efforts were made to minimise the number of animals used and minimise the pain and discomfort of the animals.

The mice used for this project represent the neurological development model closest to that of humans, as they are a widely used model proven to be representative of NPS effects (motor, sensory, cardiorespiratory and metabolic effects in an interconnected system) visible in humans (Bilel et al., 2020; Corli, Tirri, et al., 2024; Ossato et al., 2016; Vigolo et al., 2015). According to epidemiological (Bush & Woodwell, 2014; Castellanos et al., 2011) and preclinical (Wiley et al., 2019) data, males are more likely to consume SCRAs and experience intoxication from these substances. As such, the acute pharmaco-toxicological characterisation of the prophetic compound AB-5′F-BUTINACA was performed on male mice to establish a foundation for future experimental sessions involving female subjects.

Male, young adult (3–4 months old) ICR (CD-1®) mice weighing 30–35 g (Centralized Preclinical Research Laboratory, University of Ferrara, Italy) were group housed (five mice per cage; floor area per animal was 80 cm^2; minimum enclosure height was 12 cm), exposed to a 12:12 h light: dark cycle (light period from 6:30 AM to 6:30 PM) at a temperature of 20–22°C and humidity of 45%–55% and were provided ad libitum access to food (Diet 4RF25 GLP; Mucedola, Settimo Milanese, Milan, Italy) and water.

The overall study used 64 mice that were randomised for treatment. In the analysis of the behavioural responses relative to each treatment (vehicle and AB-5′F-BUTINACA at 0.1, 1 and 3 $mg{\cdot}kg^{-1}$), eight mice were used per treatment (total used mice: 32). In the analysis of the interaction of the compound with NESS0327 (0.1 $mg{\cdot}kg^{-1}$) and MDL100907 (0.1 $mg{\cdot}kg^{-1}$) and interaction of AB-5′F-BUTINACA (1 $mg{\cdot}kg^{-1}$) with either NESS0327 (0.1 $mg{\cdot}kg^{-1}$) or MDL100907 (0.1 $mg{\cdot}kg^{-1}$), eight mice were used per treatment (total used mice: 48).

2.3.2 | Drug preparation and dose selection

AB-5′F-BUTINACA was provided by Linköping University (Section 2.1), while NESS0327 and MDL100907 were purchased from Tocris (Bristol, UK). All compounds were initially dissolved in absolute ethanol (final concentration: 5%) and Tween 80 (final concentration: 2%) and brought to the final volume with saline (0.9% NaCl). The solution made with ethanol, Tween 80, and saline was also used as the vehicle. The CB_1 receptor antagonist NESS01327 (0.1 $mg{\cdot}kg^{-1}$; i.p.) and the 5-HT_{2A} receptor antagonist MDL100907 (0.1 $mg{\cdot}kg^{-1}$; i.p.) were administered 20 min before AB-5′F-BUTINACA injections. Drugs were administered by intraperitoneal injection at a volume of 4 $\mu l{\cdot}g^{-1}$. The agonist dosages were chosen based on interspecies dose scaling (Nair & Jacob, 2016) and previous studies characterising the effects of other SCRAs (Bilel et al., 2020;Corli et al., 2022; Vigolo et al., 2015) with the aim of testing concentrations that correspond to threshold, common, and high doses of SCRAs consumed by humans. The specific dose chosen to evaluate the interaction between AB-5′F-BUTINACA and antagonists was the one effective in altering sensorimotor, physiological and motor parameters in mice, without inducing major neurological changes (i.e., convulsions, hyperreflexia and myoclonia) typically observed in most of the animals injected with higher doses of SCRAs (Corli et al., 2022; Vigolo et al., 2015). The dose of NESS0327 was selected as it was previously determined to be adequate to antagonise pharmaco-toxicological effects induced by the exposure to high doses of SCRAs in mice (Bilel et al., 2023; Corli, Roda, et al., 2024). Similarly, the dose chosen for MDL100907 was reportedly adequate to antagonise sensorimotor and motor alterations observed after the injection of psychedelics (Kehne et al., 1996; Rodriguiz et al., 2021), as well as sensorimotor, antinociceptive and hypothermic effects induced by SCRAs in CD-1 mice (Corli, Tirri, et al., 2024).

2.3.3 | Behavioural tests

In the present study, the effect induced by AB-5′F-BUTINACA was investigated using a battery of behavioural tests widely used in studies of 'safety pharmacology' and routinely adopted in our laboratory for the preclinical characterisation of new SCRAs in rodents (Bilel et al., 2020; Corli, Roda, et al., 2024; Corli, Tirri, et al., 2024; Vigolo et al., 2015). To reduce the number of animals used, mice were evaluated in functional observational tests carried out in a consecutive manner according to the following time scheme: observation of visual object responses (frontal and lateral view), acoustic response, tactile response (vibrissae, corneal and pinnae reflexes) and visual placing response, rectal temperature measurement, tail pinch and tail withdrawal test, breath rate test and drag test. Behavioural tests were conducted in a thermostatic (temperature: 20–22°C, humidity: 45%–55%) and light (150 lx) controlled room with a background noise of 40 ± 4 dB. The apparatus for the visual object, acoustic, and tactile sensorimotor tests consisted of an experimental chamber (350 × 350 × 350 mm) with black methacrylate walls and a transparent front door. During the week before the experiment, each mouse was placed in the box and handled (once a day) every other day (i.e., three times total) to get used to both the environment and the experimenter. To avoid murine olfactory cues, cages were carefully cleaned with a 5%

14765381, 2026, 16, Downloaded from https://bpspubs.onlinelibrary.wiley.com/doi/10.1111/bph.70457 by Universita Di Ferrara, Wiley Online Library on [20/10/2026]. See the Terms and Conditions (https://onlinelibrary.wiley.com/terms-and-conditions) on Wiley Online Library for rules of use; OA articles are governed by the applicable Creative Commons License

ethanol solution and rinsed with water. All experiments were performed from 08:30–14:30 and conducted blindly by trained observers working in pairs (Vigolo et al., 2015). The behaviour of mice was videotaped by a camera (B/W USB Camera day&night with varifocal lens; Ugo Basile, Italy) placed at the top or on one side of the box and analysed off-line by a different trained operator. The physical condition of the mouse (e.g., body condition score) was constantly monitored by trained operators who were instructed to intervene (e.g., increased monitoring or euthanasia) and terminate, minimise or reduce pain or distress according to predetermined and specific criteria (humane endpoints; licence no. 223/2021-PR). At the end of the experiments, mice were humanely killed by cervical dislocation.

Neurological changes

As described in earlier studies (Canazza et al., 2016; Ossato et al., 2016; Vigolo et al., 2015), tail elevation, hyperreflexia, myoclonus and convulsions were observed immediately after AB-5′F-BUTINACA administration. Rapid, global contraction of all muscles on both sides of the body (legs, torso, neck, ear and facial muscles) at the same time followed by muscle relaxation was considered a medium-light myoclonic convulsion. Further, a rapid contraction of all muscles paired with a continuous and rapid 'jump' and overturning of the mouse onto its back was considered a severe convulsion. While myoclonus typically arises spontaneously in mice, convulsions can occur both spontaneously and after handling following the injection of SCRAs. Hyperreflexia was evaluated by gently stimulating the tail (one touch) to cause a reflex typically described as the exaggerated accentuation of muscle-tendon reflexes, which is manifested by an excessive reaction to an external stimulus, characterised by rapid movements (Canazza et al., 2016). Stereotypic behaviour is defined as repeated and invariant movements without any obvious goal or function (Mason, 1991). The tail elevation was measured during the observation of the freely moving mice in a square area and scored as follows: absence of tail elevation (score 0/4) and elevation of the tail from the ground surface with an inclination from 0° to 15° (score 1/4), 15° to 70° (score 2/4), 70° to 90° (score 3/4) and greater than 90° (score 4/4). Further, neurological changes are expressed as frequency (percent of animals that develop symptoms), duration (total time in minutes), and latency (time in minutes of symptom onset). Observation of neurological changes was performed at each time point considered (0, 5, 30, 60, 120, 180, 240 and 300 min post-injection) to determine duration and latency of the effects.

Evaluation of the visual response in stationary (visual object) and dynamic (visual placing) conditions

The *visual object response* test was used to evaluate the ability of the mouse to see an object approaching from the front (frontal view) or the side (lateral view) that typically induces the animal to shift or turn the head and bring the forelimbs in the 'defence' position or retreat. For the frontal visual response, a white horizontal bar was moved frontally to the mouse head, and the manoeuvre was repeated three times. For the lateral visual response, a small dentist's mirror was moved into the mouse's field of view in a horizontal arc until the stimulus was between the mouse's eyes. The procedure was conducted bilaterally (Ossato et al., 2016) and repeated three times. The score assigned was 1 if there was a reflection in the mouse movement or 0 if it was not present. The total value was calculated by adding the scores obtained in the frontal and lateral visual object response tests (overall possible score: 9). Visual object responses were evaluated at 10, 30, 60, 120, 180, 240 and 300 min post-injection.

The *visual placing response* test was performed using a tail suspension modified apparatus able to bring the mouse down towards the floor at a constant speed of 10 $cm \cdot s^{-1}$ (Ossato et al., 2016). Briefly, CD-1 mice were suspended 20 cm above the floor by an adhesive tape that was placed approximately 1 cm from the tip of the tail. The downward movement of the mouse was videotaped by a camera (B/W USB Camera day&night with varifocal lens) placed at the base of the tail suspension apparatus. Movies were analysed off-line by a trained operator who was unaware of the drug treatments administered. The frame-by-frame analysis allowed us to evaluate the beginning of the reaction of the mouse while it was approaching the floor. The first movement of the mouse when it perceives the floor is the extension of the front legs. When the mouse started the reaction, an electronic ruler evaluated the perpendicular distance in millimetres between the eyes of the mice and the floor. Untreated control mice typically perceive the floor and prepare to contact at a distance of about 23.6 ± 4.8 mm. Visual placing responses were evaluated at 15, 40, 70, 130, 190, 250 and 310 min post-injection.

Evaluation of acoustic response

Acoustic response measures the reflex of the mouse in response to an acoustic stimulus produced behind the animal (Bilel et al., 2020; Ossato et al., 2016). Four acoustic stimuli of different intensity and frequency were tested: a snap of the fingers (four snaps repeated in 1.5 s), a sharp click (produced by a metal instrument; four clicks repeated in 1.5 s), an acute sound (produced by an audiometer; frequency: 5.0–5.1 kHz) and a severe sound (produced by an audiometer; frequency: 125–150 Hz). Each test was repeated three times. The score assigned was 1 if there was a response or 0 if it was not present, for a total possible score of 3 for each sound. The acoustic total score was calculated by adding the scores obtained in the four tests (overall score: 12). The background noise (about 40 ± 4 dB) and the sound from the instruments were measured with a digital sound level meter. Acoustic responses were evaluated at 10, 30, 60, 120, 180, 240 and 300 min post-injection.

Evaluation of tactile response

Tactile response in the mouse was verified through vibrissae, corneal, and pinnae reflexes (Bilel et al., 2020; Ossato et al., 2016). Data are expressed as the sum of the three above-mentioned parameters. *Vibrissae reflex* was evaluated by touching vibrissae (right and left) with a thin hypodermic needle once per side giving a value of 1 if there was a reflex (turning of the head to the side of touch or vibrissae movement) or 0 if not present (overall possible score: 2). *Corneal reflex* was assessed by gently touching the cornea of the mouse with a thin hypodermic needle and evaluating the response. The procedure was

14765381, 2026, 16, Downloaded from https://bpspubs.onlinelibrary.wiley.com/doi/10.1111/bph.70457 by Universita Di Ferrara, Wiley Online Library on [20/10/2026]. See the Terms and Conditions (https://onlinelibrary.wiley.com/terms-and-conditions) on Wiley Online Library for rules of use; OA articles are governed by the applicable Creative Commons License

conducted bilaterally and the score assigned was 1 if the mouse moved only the head, 2 if it only closed the eyelid, and 3 if it closed the lid and moved the head (overall possible score: 6). *Pinna reflex* was assessed by touching pavilions (left and right) with a thin hypodermic needle: first the interior pavilions and then the external. This test was repeated twice for each side, giving a score of 1 if a reflex was present and 0 if it was not present (overall possible score: 4). Overall tactile responses were evaluated at 10, 30, 60, 120, 180, 240 and 300 min post-injection.

Evaluation of pain induced by mechanical (tail pinch) and thermal (tail withdrawal) stimulation of the tail

The *tail pinch* test was used to study the acute mechanical nociception (Vigolo et al., 2015). A special rigid probe connected to a digital dynamometer (ZP-50N, IMADA, Japan) was gently placed on the tail (in the distal portion) and progressive pressure was applied. When the mouse flicked its tail, the pressure was stopped and the digital instrument saved the maximum peak of weight supported (g/force). A peak of 246 ± 10.2 g/force was considered the basal value and a cut-off (500 g/force) was set to avoid tissue damage. The test was repeated three times and the final value was calculated as the average of the three obtained scores. Acute mechanical nociception was evaluated at 35, 55, 90, 145, 205, 265, and 325 min post-injection.

The *tail withdrawal* test was used to study the acute thermal nociception (Vigolo et al., 2015). Only during the execution of the test, mice were restrained in a dark plastic cylinder closed at both sides with plastic mesh, which allowed them to breathe normally. Then, half of the tail was dipped in 48°C water and the latency (in seconds) that the tail was left in the water was recorded. To ensure the temperature was homogeneous, the water was mixed at a consistent, low speed using a magnetic stir bar. 2.3 ± 0.6 s was considered as basal value and a cut-off of 15 s was set to avoid tissue damage. Acute thermal nociception was evaluated at 35, 55, 90, 145, 205, 265 and 325 min post-injection.

Evaluation of the rectal temperature

The rectal temperature was measured and used as an index of total body heat. The mouse was manually restrained by a trained operator, and the rectal temperature was evaluated by a probe (1 mm diameter). This was gently inserted, after lubrication with liquid Vaseline, into the rectum of the mouse (about 2 cm) and left in position until stabilisation of the temperature (about 10 s) (Vigolo et al., 2015). The probe was connected to a digital thermometer (Cole Parmer model 8,402). A rectal temperature of 38.5°C ± 2.0°C was considered baseline. Rectal temperature was measured at 15, 45, 75, 135, 195, 255 and 315 min post-injection.

Evaluation of breath rate

For the detection of respiratory parameters, the mice were left moving freely in a cage and their respiration patterns were videotaped by a camera (B/W USB Camera day&night with varifocal lens) placed above the observation cage. This protocol allowed for minimal handling monitoring of the awake animal. The breath rate was analysed by observing the ribcage expansion in 1-min recordings (30 frames per second). A trained operator unaware of the drug treatments performed analysed the movies off-line. The frame-by-frame analysis allowed for better estimation of the number of breath rates (brpm) of the mouse evaluated, where a count of about 257 ± 11 ribcage expansions per minute was considered the basal value (Arfè et al., 2021). Breath rate was evaluated at 15, 45, 75, 135, 195, 255 and 315 min post-injection.

Drag test

Motor activity alterations were evaluated using the drag test (Ossato et al., 2016; Vigolo et al., 2015). The *drag test* measures the ability of the animal to balance their body posture with the front legs in response to an externally dynamic stimulus. The mouse was lifted by the tail, leaving the front paws on the table, and dragged backward at a constant speed of about 20 $cm \cdot s^{-1}$ for a fixed distance (100 cm). The number of steps performed by each paw (considering 24.3 ± 3.5 steps as basal stepping activity) was recorded by two different observers. For each animal, five to seven measurements were collected (Vigolo et al., 2015). The stepping activity was evaluated at 45, 70, 105, 160, 220, 280 and 340 min post-injection.

2.3.4 | Data and statistical analysis

Data are expressed in arbitrary units for the visual object response, acoustic response, and overall tactile response and the percentage of baseline for the visual placing response, drag test, and breath rate. Rectal temperature values were expressed as the difference between control temperature (before injection) and temperature following drug administration (Δ°C). Antinociception (tail pinch and tail withdrawal tests) was calculated as the percentage of maximal effect {$E_{max}\% = [(\text{test} - \text{control latency})/(\text{cut off time} - \text{control})] \times 100$}. All data are shown as mean ± SEM of eight independent experimental replications. Statistical analysis of the effects of each compound at different concentrations over time was performed by two-way ANOVA followed by Bonferroni post hoc test for multiple comparisons. All statistical analyses were performed using the GraphPad Prism software. This study complied with the recommendations of the British Journal of Pharmacology on experimental design and analysis in pharmacology.

2.4 | Materials

Reference standards for AB-5′Br-BUTINACA, AB-5′F-BUTINACA, AB-5′Cl-BUTINACA, ADB-5′Br-BUTINACA, ADB-5′F-BUTINACA, ADB-5′Cl-BUTINACA, ADB-5′Br-PINACA, ADB-4en-5′Br-PINACA, ADB-5′Br-FUBINACA, ADB-5′Br-INACA, MDMB-5′F-BUTINACA, MMB-5′F-BUTINACA, ADB-HEXINACA, AB-HEXINACA, ADB-PINACA, ADB-4en-PINACA, AB-4en-PINACA, ADB-PropINACA (ADB-Propyl-INACA), 3OH-ADB-PropINACA, ADB-INACA, ADB-4en-PICA, ADB-

14765381, 2026, 16, Downloaded from https://bpspubs.onlinelibrary.wiley.com/doi/10.1111/bph.70457 by Universita Di Ferrara, Wiley Online Library on [20/10/2026]. See the Terms and Conditions (https://onlinelibrary.wiley.com/terms-and-conditions) on Wiley Online Library for rules of use; OA articles are governed by the applicable Creative Commons License

HEXICA, ADB-ICA, (R)-AB-4en-PICA and EMB-4en-PICA were synthesised in-house as described previously (Baginski et al., 2023; Green et al., 2025; Rautio et al., 2024).

3,5-ADB-4en-PFUPPYCA; 5F-Cumyl-Pegaclone; 5F-MDMB-PINACA; AB-CHMINACA; AB-FUBINACA; AB-PINACA; BZO-HEXOXIZID (MDA-19); JWH-018; and PB-22 were obtained from Chiron AS (Trondheim, Norway). 4CN-Cumyl-BUT7AICA, 5Cl-AB-PINACA (5-chloro ABP), ACHMINACA, ADB-5′Br-DECINACA, ADB-BUTINACA, ADB-FUBIATA, CHO-4′Me-5′Br-FUBOXPYRA and MDMB-INACA reference standards were purchased from Cayman Chemical (Ann Arbor, MI, USA). The structures of all SCRAs examined in this study can be found in Figures S1.1–S1.3.

2.5 | Nomenclature of targets and ligands

Key protein targets and ligands in this article are hyperlinked to corresponding entries in the IUPHAR/BPS Guide to PHARMACOLOGY (http://www.guidetopharmacology.org) and are permanently archived in the Concise Guide to PHARMACOLOGY 2025/26 (Alexander, Davenport, et al., 2025) GPCR.

3 | RESULTS

3.1 | AequoScreen® 5-HT$_{2A}$ and CB$_1$ intracellular Ca^{2+} release assay

The average relative efficacy values at the 5-HT$_{2A}$ receptor obtained from the screening of SCRAs (normalised to LSD) are shown in Table 1. As shown in Figure 1, the reference LSD was found to have an efficacy of 98.5% (95% CI: 96.7–100) and a potency (EC$_{50}$) of 4.85 nM (95% CI: 4.10–5.73 nM). For further comparison, mescaline was included which resulted in an efficacy of 102% (95% CI: 101–104) and EC$_{50}$ of 101 nM (95% CI: 91.7–113). Following the initial screening of 15 structurally diverse SCRAs, only two SCRAs showed some activity at the 5-HT$_{2A}$ receptor: ADB-BUTINACA and AB-HEXINACA. As only the valinamide and *tert*-leucinamide indazole- or indole-3-carboxamide SCRAs showed activity at the 5-HT$_{2A}$ receptor, 10 valinamide and 18 *tert*-leucinamide SCRAs were screened and those with an average relative efficacy over 1% of the LSD efficacy were examined further to try to obtain full concentration-response curves. As there were only two to four concentrations showing activation on the concentration-response curves, as can be seen in Figure 1, E_{max} and EC$_{50}$ values could not be calculated. Instead, as with the screening results, the average relative efficacy values of the top concentration (70 μM) are reported in Table 1. Based on the concentration-response curves, the EC$_{50}$ values were >10 μM for the tested SCRAs.

A summary of the observed structure–activity relationships (SARs) for SCRAs at 5-HT$_{2A}$ receptors is presented in Figure 2. Valinamide SCRAs showed greater activity than the *tert*-leucinamide SCRAs, indicating the less bulky isopropyl moiety on the valinamide head group produces greater activity than the *tert*-butyl moiety on the *tert*-leucinamide head group. SCRAs with an indazole core moiety were found to have greater activation of the 5-HT$_{2A}$ receptor than the indole core moiety. This can be seen from the three-fold reduction in the average relative efficacy for ADB-4en-PICA with an indole core versus ADB-4en-PINACA with an indazole core. This is opposite of the SAR for activation of the CB$_1$ receptor, where analogues with the *tert*-leucinamide head group were typically more potent and equally efficacious as analogues with the valinamide head group (Table 1).

The indazole core with a fluoride at the five position produced the greatest activity for both the valinamide and *tert*-leucinamide SCRAs, followed by the chlorinated and then the brominated core. Although the non-halogenated analogue was not available for the valinamide SCRAs, for the *tert*-leucinamide SCRAs, the chlorinated and brominated analogues showed reduced efficacy from ADB-BUTINACA, while ADB-5′F-BUTINACA had greater efficacy. In comparison, ADB-BUTINACA had similar potency and greater efficacy than its halogenated core analogues on the CB$_1$ receptor.

An examination of analogues with different tail moieties revealed that alkyl chains produce the greatest activity, where a butyl tail has the most activity, followed by propyl, then pentyl. Analogues with a hexyl chain tail (ADB-HEXINACA and AB-HEXINACA) showed almost no activity and ADB-5′Br-DECINACA with a decyl chain tail showed no activity. The pent-4-enyl tail moiety resulted in greater activity than the pentyl tail, whereas other substitutions on the alkyl chain tail, such as a terminal chloride (5Cl-AB-PINACA) and hydroxy (3OH-ADB-PropINACA), reduced the activity. This was also observed for tails with a ring, as AB-CHMINACA with a cyclohexylmethyl tail showed much greater activity than AB-FUBINACA with a fluorobenzyl tail. Tail-less analogues of *tert*-leucinamide SCRAs (ADB-5′Br-INACA, ADB-INACA and ADB-ICA) showed no activity, which was surprising as the tail-less SCRAs more closely resemble 5-HT and other common 5-HT$_{2A}$ receptor ligands.

3.2 | IP$_1$ formation 5-HT$_{2A}$ receptor activation assay

To validate the results of the AequoScreen® assay, three of the most efficacious SCRAs (AB-5′F-BUTINACA, ADB-5′F-BUTINACA and ADB-BUTINACA) were tested for 5-HT$_{2A}$ activation using an IP$_1$ formation assay. This assay uses 5-HT as reference with a resulting efficacy of 100% (95% CI: 101–104) and EC$_{50}$ of 21.1 nM (95% CI: 17.9–24.9). As shown in Figure 3, all three SCRAs also showed 5-HT$_{2A}$ receptor activation in this assay, comparable to the results obtained with the AequoScreen® assay. AB-5′F-BUTINACA and ADB-BUTINACA had similar potency (25.9 and 71.4 μM, respectively) and efficacy (60.0% and 61.2%). It should be noted that while nonlinear regression curves were able to be fitted to these data, it is not clear if these compounds have reached a plateau of maximal response, so the potency and efficacy values should be considered with caution. Unfortunately, there was not enough of the ADB-5′F-BUTINACA reference standard available to test the highest concentration (1000 μM), but its efficacy at 100 μM was 29.9%. An additional set of 20 SCRAs was screened for activation of

14765381, 2026, 16, Downloaded from https://bpspubs.onlinelibrary.wiley.com/doi/10.1111/bph.70457 by Universita Di Ferrara, Wiley Online Library on [20/10/2026]. See the Terms and Conditions (https://onlinelibrary.wiley.com/terms-and-conditions) on Wiley Online Library for rules of use; OA articles are governed by the applicable Creative Commons License

TABLE 1 Efficacy of SCRAs at the 5-HT_{2A} receptor and at the CB_1 receptor.

	Compound	5-HT_{2A} Efficacy (% LSD)	CB_1 Efficacy (% JWH-018) [95% CI]	CB_1 Potency (nM) [95% CI]
Initial Screening	ADB-BUTINACA	33.7	-	-
	AB-HEXINACA	1	-	-
	3,5-ADB-4en-PFUPPYCA	0	-	-
	4CN-Cumyl-BUT7AICA	0	-	-
	5F-Cumyl-Pegaclone	0	-	-
	5F-MDMB-PINACA	0	-	-
	ACHMINACA	0	-	-
	BZO-HEXOXIZID	0	-	-
	CHO-4′Me-5′Br-FUBOXPYRA	0	-	-
	JWH-018	0	-	-
	EMB-4en-PICA	0	-	-
	MDMB-5′Br-BUTINACA	0	-	-
	MDMB-INACA	0	-	-
	MMB-5′Br-BUTINACA	0	-	-
	PB-22	0	-	-
Valinamide	AB-5′F-BUTINACA	67.3	107 [105–110]	18.7 [15.7–22.2]
	AB-5′Cl-BUTINACA	57.4	112 [109–116]	57.7 [47.7–69.9]
	AB-5′Br-BUTINACA	39.1	115 [112–118]	44.6 [37.0–53.6]
	AB-4en-PINACA	26.6	110 [106–113]	20.1 [16.2–25.0]
	AB-CHMINACA	21.1	108 [105–111]	8.98 [7.37–10.9]
	AB-PINACA	16.4	111 [108–114]	10.3 [8.56–12.4]
	5Cl-AB-PINACA	1	111 [109–113]	34.7 [29.6–39.2]
	AB-HEXINACA	1.10	145 [142–148]	139 [121–159]
	AB-FUBINACA	1	108 [106–111]	8.94 [7.46–10.7]
	(R)-AB-4en-PICA	0	31.1[a]	ND
Tert-leucinamide	ADB-5′F-BUTINACA	32.8	113 [109–117]	14.4 [11.1–18.8]
	ADB-BUTINACA	22.3	126 [123–129]	21.5 [18.0–25.6]
	ADB-5′Cl-BUTINACA	20.1	113 [109–116]	30.1 [24.8–36.6]
	ADB-PropINACA	19.0	115 [113–117]	42.2 [37.7–47.2]
	ADB-5′Br-BUTINACA	17.2	110 [108–112]	18.0 [15.5–21.0]
	ADB-4en-PINACA	12.3	117 [115–120]	17.4 [14.0–21.6]
	ADB-PINACA	7.67	116 [114–119]	23.4 [20.0–27.3]
	ADB-HEXINACA	1	117 [115–120]	39.4 [34.6–44.8]
	ADB-4en-5′Br-PINACA	1	111 [109–114]	14.2 [12.2–16.6]
	ADB-4en-PICA	1	117 [114–120]	28.2 [23.5–33.9]
	ADB-HEXICA	1	133 [129–137]	85.9 [71.7–103]
	ADB-INACA	0	88.1[a]	ND
	3OH-ADB-PropINACA	0	93.3 [90.4–96.2]	971 [825–1140]
	ADB-5′Br-INACA	0	111 [107–115]	2290 [1960–2670]
	ADB-5′Br-DECINACA	0	4.89[a]	ND
	ADB-5′Br-FUBINACA	0	112 [109–116]	42.1 [34.6–51.2]
	ADB-ICA	0	5.89[a]	ND
	ADB-FUBIATA	0	102[a]	1281 [1036–1586]

Note: Average relative efficacy values at the 5-HT_{2A} receptor (normalised to LSD, which is arbitrarily set at 100%) and relative efficacy (E_{max}) and potency (EC_{50}) values at the CB_1 receptor (normalised to JWH-018, which is arbitrarily set at 100%) for examined SCRAs on the AequoScreen® 5-HT_{2A} and CB_1 intracellular Ca^{2+} release assays. For the initial screening of 15 structurally diverse SCRAs, the efficacy from the testing of the top concentration (70 μM) in triplicate in one experiment is reported. For the valinamide (n = 10) and *tert*-leucinamide (n = 18) SCRAs with >1% efficacy, the reported values for the 5-HT_{2A} receptor are the average of the top concentration (70 μM) from three independent experiments. Compounds are organised by descending 5-HT_{2A} efficacy.

[a]Maximal activation observed at a concentration of 60 μM. Accompanying EC_{50} values could not be calculated accurately.

ND, not determined (values could not be calculated as saturation was not reached).

14765381, 2026, 16, Downloaded from https://bpspubs.onlinelibrary.wiley.com/doi/10.1111/bph.70457 by Universita Di Ferrara, Wiley Online Library on [20/10/2026]. See the Terms and Conditions (https://onlinelibrary.wiley.com/terms-and-conditions) on Wiley Online Library for rules of use; OA articles are governed by the applicable Creative Commons License

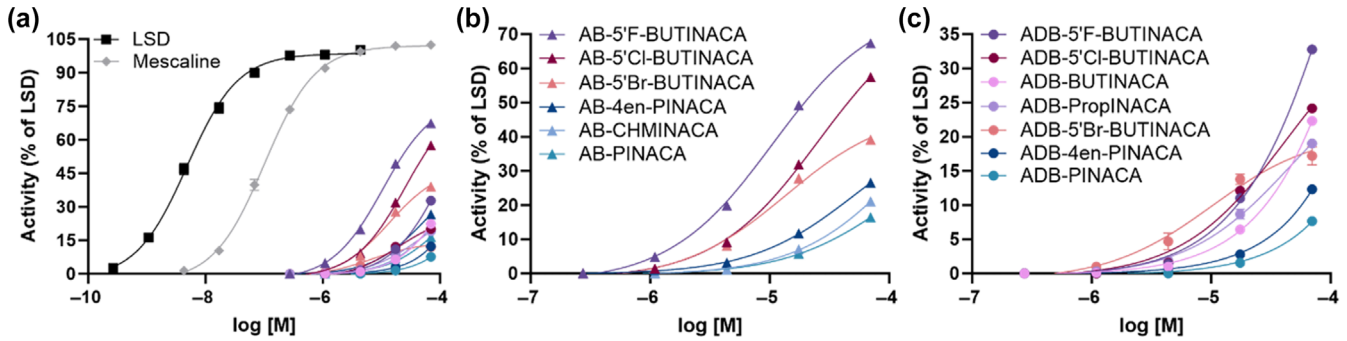


FIGURE 1 5-HT_{2A} receptor activation profiles on the AequoScreen® 5-HT_{2A} intracellular Ca^{2+} release assays for a panel of valinamide (AB) and *tert*-leucinamide (ADB) SCRAs, where (a) shows all the SCRAs alongside lysergic acid diethylamide (LSD) and mescaline for reference, (b) shows all valinamide synthetic cannabinoid receptor agonists (SCRAs) and (c) shows all *tert*-leucinamide SCRAs. All data are normalised to the maximal response of the reference standard, LSD (in black in left chart), arbitrarily set at 100%, and each datapoint represents the mean ± SEM, obtained from a minimum of three independent experiments, run in triplicate (n ≥ 3). Note the difference in scale between charts.

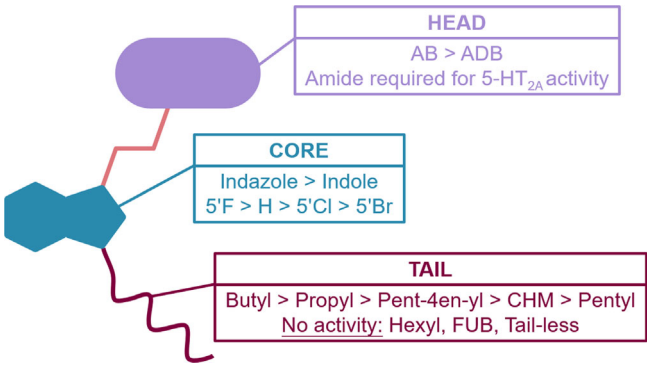


FIGURE 2 Summary of the structure–activity relationships observed for synthetic cannabinoid receptor agonists (SCRAs) on the 5-HT_{2A} receptor from evaluation of their activation profiles on the AequoScreen® 5-HT_{2A} intracellular Ca^{2+} release assays. It should be noted that many of these relationships require further evaluation.

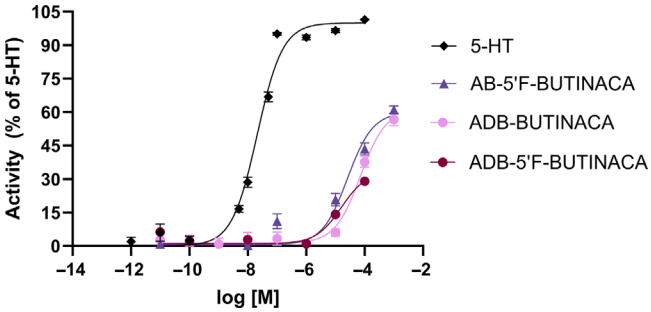


FIGURE 3 5-HT_{2A} receptor activation profiles on the inositol monophosphate (IP_1) formation assay for ADB-BUTINACA, ADB-5′F-BUTINACA and AB-BUTINACA in comparison to 5-HT. All data are normalised to the maximal response of the reference standard 5-HT (in black), arbitrarily set at 100%, and each datapoint represents the mean ± SEM obtained from a minimum of three independent experiments.

the 5-HT_{2A} receptor using fluorescence imaging plate reader (FLIPR)-based calcium mobilisation and radioligand binding assays, where only AB-FUBINACA showed some binding affinity (see Table S2.1).

3.3 | In vivo results

None of the behavioural tests were changed in vehicle-, NESS0327-, or MDL100907-treated mice over the observation period. Conversely, the injection of AB-5′F-BUTINACA induced significant behavioural and neurological changes (Table S3.1).

3.3.1 | Neurological changes

In this study, persistent circling (full 360° rotation) was observed, which is a stereotypic behaviour (i.e., repeated, persistent behaviour) (Campos-Ordoñez et al., 2022). Increased frequency, latency, and duration of the effect were observed at higher doses (1–3 $mg \cdot kg^{-1}$). The highest dose of AB-5′F-BUTINACA (3 $mg \cdot kg^{-1}$) induced spontaneous and handling-induced convulsions and hyperreflexia, which were not observed at lower doses (0.1 and 1 $mg \cdot kg^{-1}$). However, both 1 and 3 $mg \cdot kg^{-1}$ of the compound increased the degree of tail elevation in 66% and 50% of mice, respectively. We did not observe any head-twitch response (typically used to measure the hallucinogenic potential of 5-HT_{2A} receptor agonists) following the injection of the drug. All neurological changes were prevented by pretreatment with the selective CB_1 receptor antagonist NESS0327 (1 $mg \cdot kg^{-1}$) and the selective 5-HT_{2A} receptor antagonist MDL100907 (0.1 $mg \cdot kg^{-1}$; Table 2).

3.3.2 | Evaluation of the visual object response

Systemic administration of AB-5′F-BUTINACA (1–3 $mg \cdot kg^{-1}$) induced a deep but transitory decrease of the visual object response (Figure 4a). The visual object reflex was restored by pretreatment with the CB_1 antagonist NESS0327 (1 $mg \cdot kg^{-1}$) (Figure 4b) and the 5-HT_{2A} antagonist MDL100907 (0.1 $mg \cdot kg^{-1}$) (Figure 4c).

14765381, 2026, 16, Downloaded from https://bpspubs.onlinelibrary.wiley.com/doi/10.1111/bph.70457 by Universita Di Ferrara, Wiley Online Library on [20/10/2026]. See the Terms and Conditions (https://onlinelibrary.wiley.com/terms-and-conditions) on Wiley Online Library for rules of use; OA articles are governed by the applicable Creative Commons License

3.3.3 | Evaluation of the visual placing response

Systemic administration of AB-5′F-BUTINACA (0.1–3 mg·kg^{-1}) induced a deep and prolonged decrease of the visual placing response (Figure 4d). Pretreatment with the CB_1 antagonist NESS0327 (1 mg·kg^{-1}) prevented the effect induced by the agonist (Figure 4e). The visual placing reflex was partially restored by pretreatment with the 5-HT_{2A} antagonist MDL100907 (0.1 mg·kg^{-1}) in AB-5′F-BUTINACA-treated mice at 15 min, while it was totally restored starting from 35 min after the injection (Figure 4f).

3.3.4 | Evaluation of the acoustic response

Systemic administration of AB-5′F-BUTINACA (0.1–3 mg·kg^{-1}) induced a transitory decrease of the acoustic reflex (Figure 5a). The acoustic reflex was restored by pretreatment with the CB_1 antagonist NESS0327 (1 mg·kg^{-1}) (Figure 5b). Similarly, pretreatment with the 5-HT_{2A} antagonist MDL100907 (0.1 mg·kg^{-1}) prevented the effect on acoustic response (Figure 5c).

3.3.5 | Evaluation of the overall tactile reflex

Systemic administration of AB-5′F-BUTINACA (1–3 mg·kg^{-1}) induced a transitory decrease of the overall tactile reflex (Figure 5d). The overall tactile responses were restored by pretreatment with the CB_1 antagonist NESS0327 (1 mg·kg^{-1}) (Figure 5e). Similarly, pretreatment with the 5-HT_{2A} antagonist MDL100907 (0.1 mg·kg^{-1}) prevented the effect induced on overall tactile response (Figure 5f).

3.3.6 | Evaluation of pain induced by a mechanical stimulus

Systemic administration of AB-5′F-BUTINACA induced a transitory (0.1–1 mg·kg^{-1}) or long-lasting (3 mg·kg^{-1}) increase of the latency to the tail flick response evoked by the acute mechanical pain stimulus in mice (Figure 6a). The antinociceptive effect provoked by the agonist was partly prevented by pretreatment with the CB_1 antagonist NESS0327 (1 mg·kg^{-1}) at 35 min after the injection (Figure 6b), but not by pretreatment with the 5-HT_{2A} antagonist MDL100907 (0.1 mg·kg^{-1}) (Figure 6c).

3.3.7 | Evaluation of pain induced by a thermal stimulus

Systemic administration of AB-5′F-BUTINACA induced a long-lasting (1–3 mg·kg^{-1}) increase of the latency to the tail flick response evoked by the acute thermal pain stimulus in mice (Figure 6d). The control group did not reveal a hyperalgesia effect at various time points. The antinociceptive effect provoked by the agonist was prevented by pretreatment with the CB_1 antagonist NESS0327 (1 mg·kg^{-1}) up to 205 min after the injection (Figure 6e). Pretreatment with the 5-HT_{2A} antagonist MDL100907 (0.1 mg·kg^{-1}) prevented the effect from 55 to 205 min (Figure 6f).

TABLE 2 Neurological effects of AB-5′F-BUTINACA and interactions with CB_1 receptor antagonist and 5-HT_{2A} receptor antagonist.

		Treatment				
Neurological changes		AB-5′F-BUTINACA 0.1 mg·kg^{-1}	AB-5′F-BUTINACA 1 mg·kg^{-1}	AB-5′F-BUTINACA 3 mg·kg^{-1}	AB-5′F-BUTINACA + NESS0327	AB-5′F-BUTINACA + MDL100907
Tail elevation	Frequency (%)	-	66	50	-	-
	Score	-	1.66 ± 0.58	2.33 ± 0.58	-	-
	Duration (min)	-	180	180	-	-
	Latency (min)	-	60	5	-	-
Stereotypies	Frequency (%)	80	100	100	-	-
	Duration (min)	60	120	180	-	-
	Latency (min)	5	5	30	-	-
Hyperreflexia	Frequency (%)	-	-	100	-	-
	Duration (min)	-	-	30	-	-
	Latency (min)	-	-	5	-	-
Convulsions	Frequency (%)	-	-	100	-	-
	Duration (min)	-	-	30	-	-
	Latency (min)	-	-	5	-	-

Note: Neurological changes were observed after the injection of AB-5′F-BUTINACA (0.1–3 mg·kg^{-1}; i.p.) and interaction with the selective CB_1 receptor antagonist NESS0327 (1 mg·kg^{-1}; i.p.) and the 5-HT_{2A} selective receptor antagonist MDL100907 (0.1 mg·kg^{-1}; i.p.). The injection of vehicle, NESS0327, or MDL100907 alone did not modify the neurological functions in mice. Data are expressed as percentage (frequency of animal with neurological signs), minutes (duration and latency of neurological signs) and score (degree of elevation connected to the elevation of the tail). The tail elevation score assessment represents the mean ± SEM of six animals for each treatment.

14765381, 2026, 16, Downloaded from https://bpspubs.onlinelibrary.wiley.com/doi/10.1111/bph.70457 by Universita Di Ferrara, Wiley Online Library on [20/10/2026]. See the Terms and Conditions (https://onlinelibrary.wiley.com/terms-and-conditions) on Wiley Online Library for rules of use; OA articles are governed by the applicable Creative Commons License

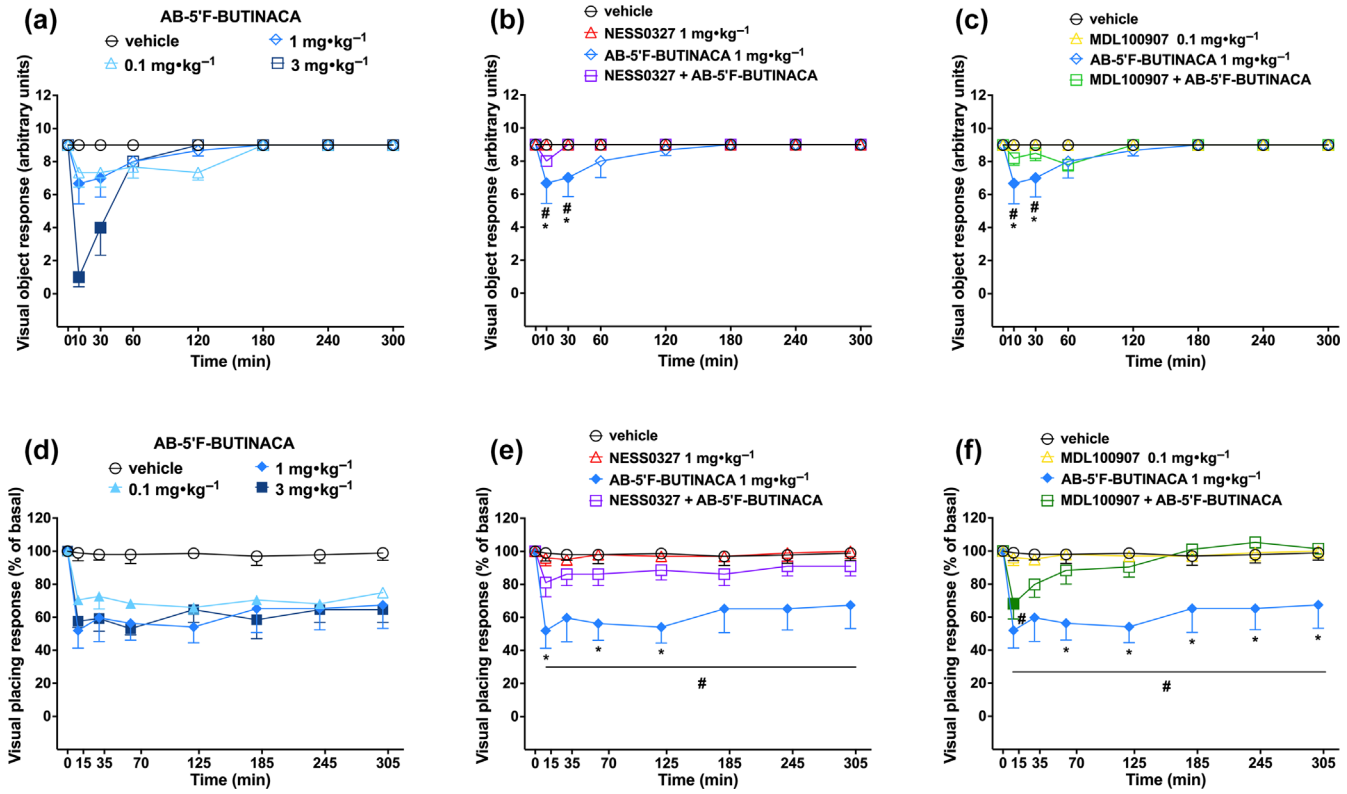


FIGURE 4 Effect of AB-5′F-BUTINACA (0.1–3 mg·kg^{-1}; i.p.) administration on the visual object (a–c) and placing (d–f) test in mice. Data are expressed as arbitrary units (a–c) and as percentage of baseline (d–f) and represent the mean ± SEM of 6 determinations for each treatment. Interaction of AB-5′F-BUTINACA (1 mg·kg^{-1}; i.p.) with the selective CB_1 receptor antagonist NESS0327 (1 mg·kg^{-1}; i.p.) and the selective $5HT_{2A}$ receptor antagonist MDL100907 (0.1 mg·kg^{-1}; i.p.) is reported in (b) and (e) and (c) and (f), respectively. Data with filled symbols show significant ($P < 0.05$) difference from vehicle; $^{\#}P < 0.05$, significantly different from antagonist alone; $^{*}P < 0.05$, significantly different from antagonist + AB-5′F-BUTINACA; two-way ANOVA followed by Bonferroni's test for multiple comparisons.

3.3.8 | Evaluation of rectal temperature

Systemic administration of AB-5′F-BUTINACA (3 mg·kg^{-1}) induced transitory hypothermia between 30 and 50 min after the injection (Figure 7a). The rectal temperature of AB-5′F-BUTINACA-treated mice was not affected by pretreatment with the CB_1 antagonist NESS0327 (1 mg·kg^{-1}) (Figure 7b). On the other hand, pretreatment with the 5-HT_{2A} antagonist MDL100907 provoked transitory hypothermia in mice at 30 min, while the rectal temperature gradually returned to baseline starting from 50 min after the injection (Figure 7c).

3.3.9 | Evaluation of breath rate

Systemic administration of AB-5′F-BUTINACA (1–3 mg·kg^{-1}) promptly and deeply reduced breath rate of mice starting from 15 min after the injection and lasting up to 65 min (Figure 7d). Reduction of breath rate induced by the agonist was not prevented by pretreatment with the CB_1 antagonist NESS0327 (1 mg·kg^{-1}) (Figure 7e) or the 5-HT_{2A} antagonist MDL100907 (0.1 mg·kg^{-1}) (Figure 7f).

3.3.10 | Evaluation of number of steps

In line with the decreased motor activity pattern observed after the systemic administration of AB-5′F-BUTINACA (1 mg·kg^{-1}), ANOVA analysis highlighted a brief and transitory reduction of the number of steps at 220 min after the injection (Figure 8a). The inhibitory effect was prevented by pretreatment with the CB_1 receptor antagonist NESS0327 (1 mg·kg^{-1}) (Figure 8b). On the other hand, pretreatment with the 5-HT_{2A} receptor antagonist MDL100907 (0.1 mg·kg^{-1}) provoked a reduction in the number of steps of AB-5′F-BUTINACA-treated mice between 45 and 220 min (Figure 8c).

4 | DISCUSSION

This study aimed to further understand the adverse effect profiles of SCRAs that are suspected to be mediated by non-cannabinoid targets. Interactions of SCRAs with the dopaminergic (Ossato et al., 2017) and serotonergic systems have been proposed (Fantegrossi et al., 2018). Our findings provide the first evidence of the involvement of 5-HT_{2A} receptors in the mechanisms underlying some of the acute effects and

14765381, 2026, 16, Downloaded from https://bpspubs.onlinelibrary.wiley.com/doi/10.1111/bph.70457 by Universita Di Ferrara, Wiley Online Library on [20/10/2026]. See the Terms and Conditions (https://onlinelibrary.wiley.com/terms-and-conditions) on Wiley Online Library for rules of use; OA articles are governed by the applicable Creative Commons License

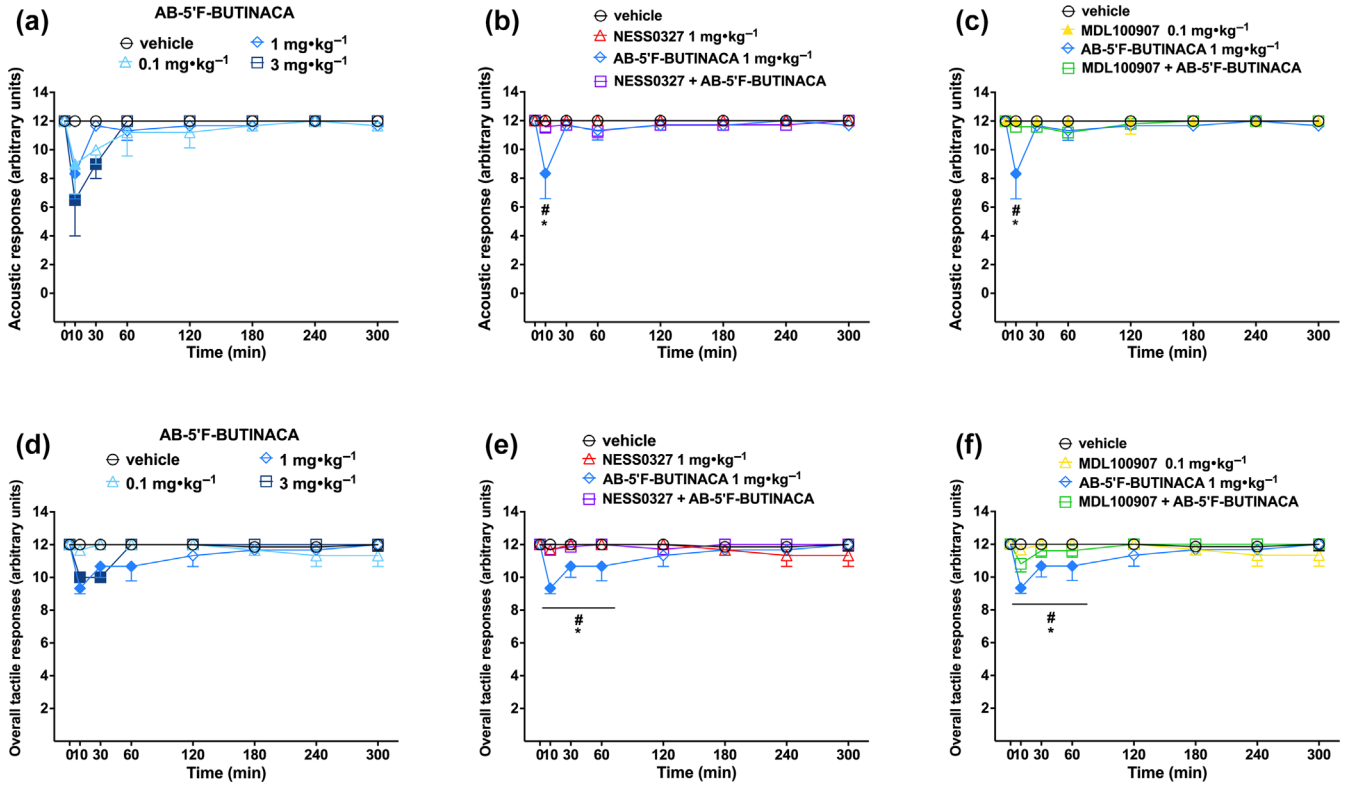


FIGURE 5 Effect of AB-5′F-BUTINACA (0.1–3 mg·kg^{-1}; i.p.) administration on the acoustic (a–c) and overall tactile (d–f) response in mice. Data are expressed as arbitrary units (a–f) and represent the mean ± SEM of 6 determinations for each treatment. The interaction of AB-5′F-BUTINACA (1 mg·kg^{-1}; i.p.) with the selective CB_1 receptor antagonist NESS0327 (1 mg·kg^{-1}; i.p.) and the selective $5HT_{2A}$ receptor antagonist MDL100907 (0.1 mg·kg^{-1}; i.p.) is reported in (b) and (e) and (c) and (f), respectively. Data with filled symbols show significant ($P < 0.05$) difference from vehicle; $^{\#}P < 0.05$, significantly different from antagonist alone; $^{*}P < 0.05$, significantly different from antagonist + AB-5′F-BUTINACA; two-way ANOVA followed by Bonferroni's test for multiple comparisons.

related risk of the use of newly emerging SCRAs. Previous studies assessing dopaminergic and serotonergic involvement have been conducted for earlier generation SCRAs, for example, AKB-48 (APINACA) and JWH-018 (Corli, Tirri, et al., 2024; Ossato et al., 2017; Yano et al., 2020). In the present study, diverse classes of earlier and newer generation SCRAs were screened for activity at the 5-HT_{2A} receptor. Some direct activation by indole and indazole SCRAs with valinamide and *tert*-leucinamide head moieties was found, including activation by the widely abused and popular SCRA ADB-BUTINACA (Kronstrand et al., 2022; Monti et al., 2025). The greatest efficacy at 5-HT_{2A} receptors was exhibited by the prophetic SCRA AB-5′F-BUTINACA, which reached 67.3% efficacy of LSD at the highest tested concentration of 70 μM in the AequoScreen® assay. These results were reproducible using a second distinct bioassay for AB-5′F-BUTINACA, ADB-BUTINACA and ADB-5′F-BUTINACA.

As only SCRAs with a valinamide or *tert*-leucinamide head moiety showed activity at the 5-HT_{2A} receptor, the amide in the head moiety is likely to be required for activation. This is supported by the presence of an amine group in many of the well-known potent 5-HT_{2A} receptor agonists, including 5-HT, LSD, psilocin and mescaline. A change in the *N*,*N*-diethylamide moiety of LSD significantly reduced the in vivo potency, indicating the 5-HT_{2A} receptor has a region accommodating the diethylamide moiety that is stereochemically defined and sterically constrained (Nichols, 2012). This is supported by structure–function studies that have found the terminal amine moiety of psychedelics is anchored in the 5-HT_{2A} receptor by a transmembrane helix III aspartic acid (Asp-155) (Kristiansen et al., 2000). In addition, in silico modelling of LSD bound to the 5-HT_{2A} receptor showed that the amide carbonyl oxygen accepts a hydrogen bond from a residue at the extracellular end of transmembrane segment 6 of the 5-HT_{2A} receptor (Chambers & Nichols, 2002). In silico modelling of arylpiperazine derivatives with an amide linking group at the 5-HT_{2A} receptor also found that the NH of the amide group plays an important role in donating hydrogen to form a hydrogen bond interaction with the receptor, which promotes the potency (F. Lin et al., 2017).

Valinamide SCRAs showed greater activity than the *tert*-leucinamide SCRAs. The opposite relationship was observed for the CB_1 receptor, where the *tert*-leucinamide SCRAs were more potent, which has also been found by other studies (Grafinger et al., 2021; Green et al., 2025; Noble et al., 2019). On the other hand, similar to CB_1 receptor activity, the indazole core analogues were more active than the indole core analogues. This was unexpected as it was presumed that SCRAs with an indole core moiety would produce greater activation of the 5-HT_{2A} receptor, given that 5-HT has an indole structure. Unfortunately, there were few indole analogues of

14765381, 2026, 16, Downloaded from https://bpspubs.onlinelibrary.wiley.com/doi/10.1111/bph.70457 by Universita Di Ferrara, Wiley Online Library on [20/10/2026]. See the Terms and Conditions (https://onlinelibrary.wiley.com/terms-and-conditions) on Wiley Online Library for rules of use; OA articles are governed by the applicable Creative Commons License

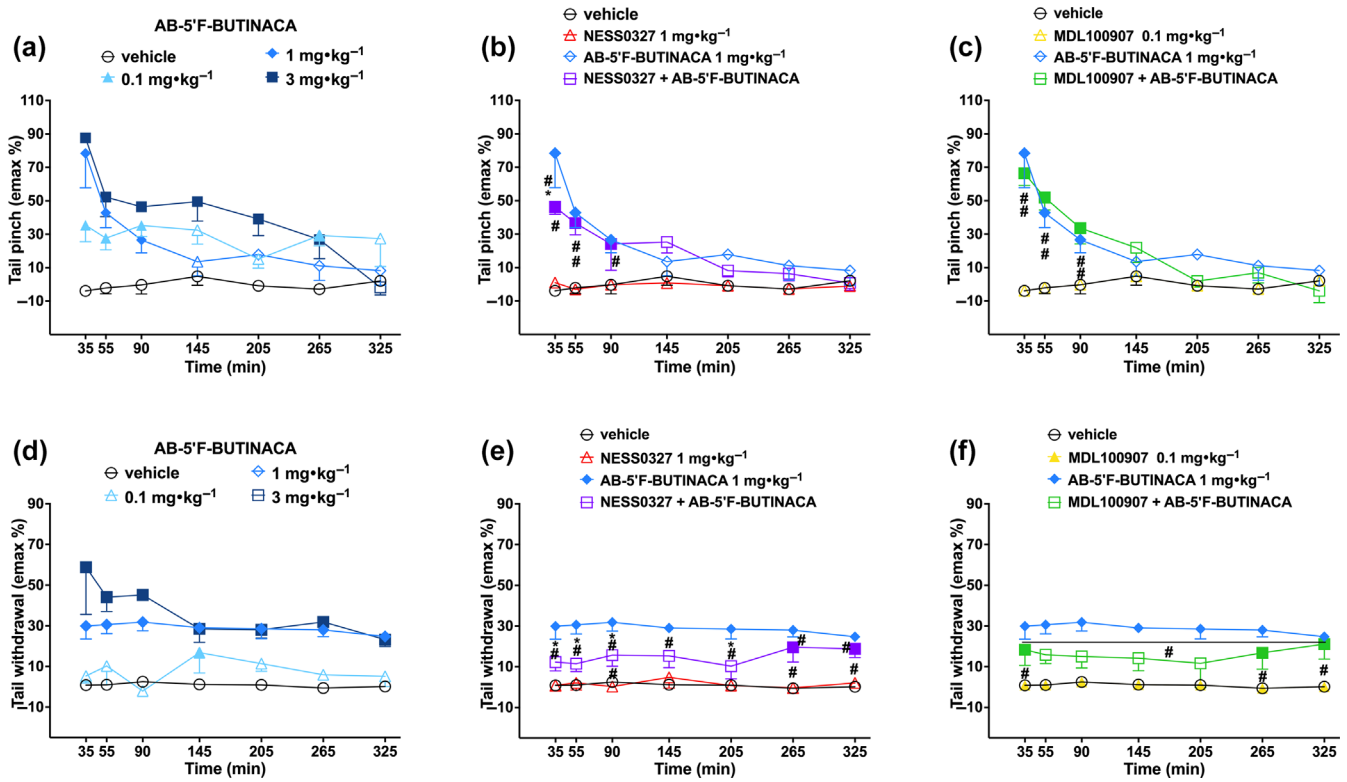


FIGURE 6 Effect of AB-5′F-BUTINACA (0.1–3 mg·kg^{-1}; i.p.) administration on the tail pinch (a–c) and tail withdrawal (d–f) in mice. Data are expressed as percentage of maximal effect (a–f) and represent the mean ± SEM of 6 determinations for each treatment. The interaction of AB-5′F-BUTINACA (1 mg·kg^{-1}; i.p.) with the selective CB_1 receptor antagonist NESS0327 (1 mg·kg^{-1}; i.p.) and the selective 5-HT_{2A} receptor antagonist MDL100907 (0.1 mg·kg^{-1}; i.p.) is reported in (b) and (e) and (c) and (f), respectively. Data with filled symbols show significant ($P < 0.05$) difference from vehicle; $^{\#}P < 0.05$, significantly different from antagonist alone; $^{*}P < 0.05$, significantly different from antagonist + AB-5′F-BUTINACA; two-way ANOVA followed by Bonferroni's test for multiple comparisons.

valinamide and *tert*-leucinamide SCRAs available for testing, so this relationship should be explored further with more indole analogues with tail groups that exhibit greater activity, such as AB- and ADB-BUTICA. Finally, for the halogenated indazole cores, the average relative efficacy decreased as the mass of the halogen increased and electronegativity decreased, except for ADB-BUTINACA which had greater efficacy than its analogues with a chlorinated and brominated core. As 5-HT itself has a hydroxy group at the 5-position on the indole core, it would be interesting to test analogues of AB- and ADB-BUTINACA with a hydroxy group at the 5-position to see how they compare to the halogenated core.

In contrast to the detected activation in the nM range for the CB_1 receptor, the tested SCRAs have EC_{50} values at the 5-HT_{2A} receptor in the μM range (>10 μM), which suggests that the direct activation of these SCRAs may not be pharmacologically relevant. However, recent studies have found the involvement of 5-HT_{2A} receptor activation in vivo, including SCRAs that showed no activation with the presented in vitro models, such as JWH-018 (Corli, Tirri, et al., 2024). Hence, the most efficacious SCRA found in this study, AB-5′F-BUTINACA, was evaluated in vivo to determine its physiological relevance. The in vivo evaluation revealed that systemic injection of AB-5′F-BUTINACA leads to severe pharmaco-toxicological effects. The highest doses (1–3 mg·kg^{-1}) induced notable neurological changes, as well as sensorimotor, physiological (hypothermia and bradypnea), nociceptive, and motor disruptions in mice. These findings are consistent with previous studies evaluating the toxicity of different generations of SCRAs in rodents (Canazza et al., 2016; Ossato et al., 2016; Vigolo et al., 2015) and demonstrate that this compound can provoke alterations attributable to the typical 'tetrad effect' (i.e., analgesia, hypothermia, catalepsy and suppressed locomotion) (Metna-Laurent et al., 2018).

The highest dose of AB-5′F-BUTINACA resulted in major neurological changes, including convulsions and hyperreflexia, which agree with preclinical data (Canazza et al., 2016; Vigolo et al., 2015) but also clinical reports chronicling seizure-like activity in humans after exposure to scheduled SCRAs (Abouchedid et al., 2017; Schep et al., 2015). In line, the neurological effects (e.g., elevation of the tail and stereotyped behaviour) evoked by 1 mg·kg^{-1} of the tested compound were prevented by pretreatment with the CB_1 receptor antagonist NESS0327. The prior injection of the 5-HT_{2A} receptor antagonist MDL100907 also prevented these changes, suggesting the involvement of 5-HT receptor-mediated mechanisms. Further, Amodeo et al. have shown that micro-infusion of the same antagonist in the dorsomedial striatum attenuated stereotyped behaviour observed in a BTBR mouse model of autism suggesting that 5-HT receptors are involved in stereotypies of diverse nature (Amodeo et al., 2017).

14765381, 2026, 16, Downloaded from https://bpspubs.onlinelibrary.wiley.com/doi/10.1111/bph.70457 by Universita Di Ferrara, Wiley Online Library on [20/10/2026]. See the Terms and Conditions (https://onlinelibrary.wiley.com/terms-and-conditions) on Wiley Online Library for rules of use; OA articles are governed by the applicable Creative Commons License

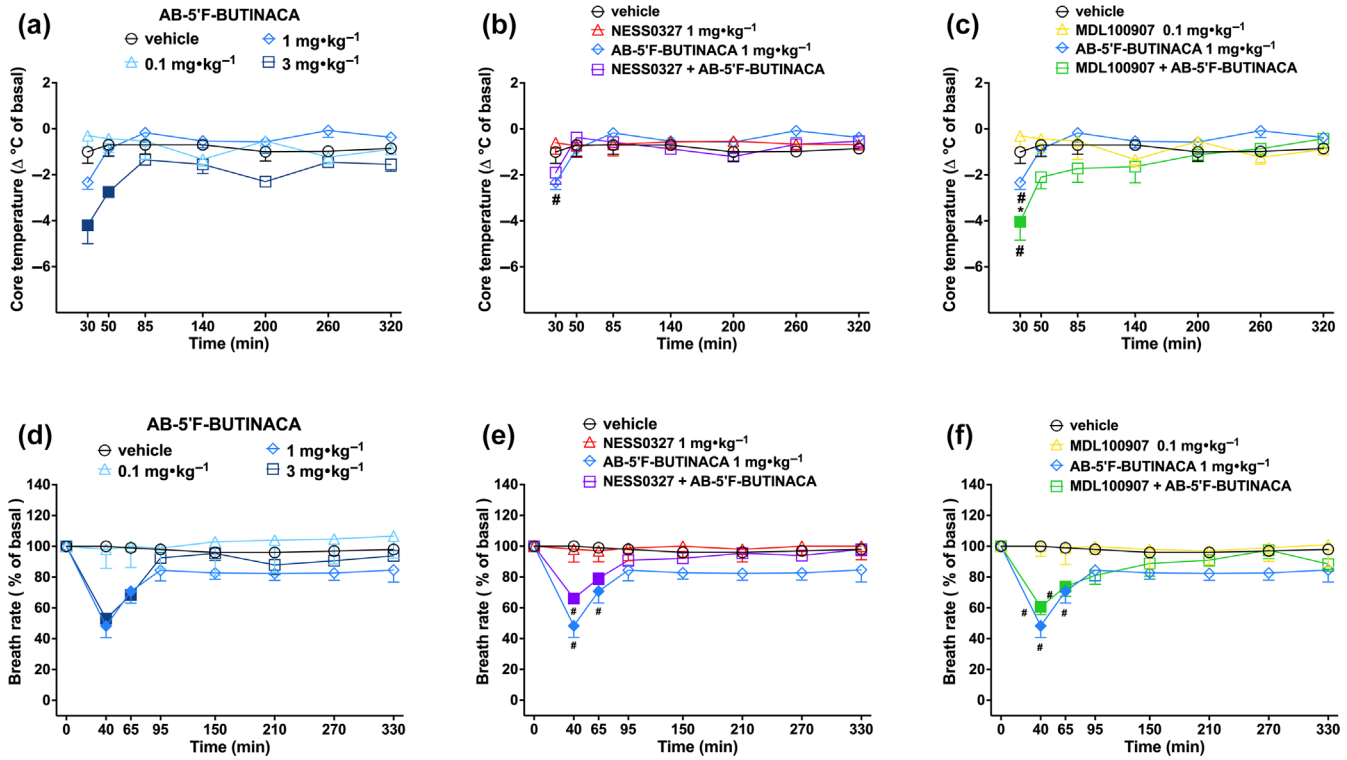


FIGURE 7 Effect of AB-5′F-BUTINACA (0.1–3 mg·kg^{-1}; i.p.) administration on the rectal temperature (a–c) and breath rate (d–f) in mice. Data are expressed as Δ°C (a–c) and percentage of baseline (d–f) and represent the mean ± SEM of 6 determinations for each treatment. Interaction of AB-5′F-BUTINACA (1 mg·kg^{-1}; i.p.) with the selective CB_1 receptor antagonist NESS0327 (1 mg·kg^{-1}; i.p.) and the selective 5-HT_{2A} receptor antagonist MDL100907 (0.1 mg·kg^{-1}; i.p.) is reported in (b) and (e) and (c) and (f), respectively. Data with filled symbols show significant ($P < 0.05$) difference from vehicle; $^{\#}P < 0.05$, significantly different from antagonist alone; $^{*}P < 0.05$, significantly different from antagonist + AB-5′F-BUTINACA; two-way ANOVA followed by Bonferroni's test for multiple comparisons.

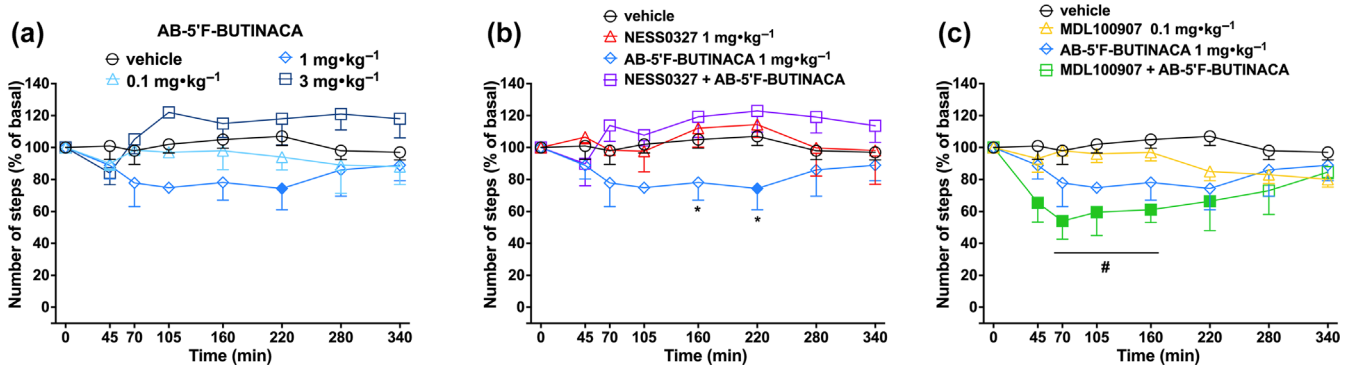


FIGURE 8 Effect of AB-5′F-BUTINACA (0.1–3 mg·kg^{-1}; i.p.) administration on the drag test (a–c) in mice. Data are expressed as percentage of baseline and represent the mean ± SEM of 6 determinations for each treatment. The interaction of AB-5′F-BUTINACA (1 mg·kg^{-1}; i.p.) with the selective CB_1 receptor antagonist NESS0327 (1 mg·kg^{-1}; i.p.) and the selective 5-HT_{2A} receptor antagonist MDL100907 (0.1 mg·kg^{-1}; i.p.) is reported in (c) and (d), respectively. Data with filled symbols show significant ($P < 0.05$) difference from vehicle; $^{\#}P < 0.05$, significantly different from antagonist alone; $^{*}P < 0.05$, significantly different from antagonist + AB-5′F-BUTINACA; two-way ANOVA followed by Bonferroni's test for multiple comparisons.

Further, antagonising the CB_1 and 5-HT_{2A} receptors restored the visual, acoustic, and tactile responses in AB-5′F-BUTINACA-treated mice. To date, evidence on the key role played by the interaction between cannabinoid and 5-HT receptors in triggering SCRA-induced sensorimotor disruption has emerged (Corli, Tirri, et al., 2024). A previous study linked chronic treatment with Δ^9-THC to the enhancement of the pro-psychedelic signalling of 5-HT_{2A} receptors in the young mouse brain cortex (Ibarra-Lecue et al., 2018). Thus, the present results suggest that AB-5′F-BUTINACA can induce notable disruption to sensory information processing. In the translational

14765381, 2026, 16, Downloaded from https://bpspubs.onlinelibrary.wiley.com/doi/10.1111/bph.70457 by Universita Di Ferrara, Wiley Online Library on [20/10/2026]. See the Terms and Conditions (https://onlinelibrary.wiley.com/terms-and-conditions) on Wiley Online Library for rules of use; OA articles are governed by the applicable Creative Commons License

paradigm, this is consistent with the altered visual and auditory perceptions associated with psychotic conditions that have been reported in patients exposed to SCRAs (Kak et al., 2017).

AB-5′F-BUTINACA increased the threshold for acute mechanical pain stimulus in mice. Pretreatment with the CB_1 antagonist NESS0327 or the 5-HT_{2A} antagonist MDL100907 did not prevent the effect, except for a temporary (35 min post-injection) restoration of the nociceptive reflex in NESS0327-pretreated mice. A previous study of the effects of Δ^9-THC showed that the antinociceptive effects of cannabinoids are not modulated by heterodimeric 5-HT_{2A}/CB_1 receptors in the brain of rodents (Viñals et al., 2015). Moreover, Wang et al. recently suggested the involvement of **CB_2 receptors** in altering nociception in mice (Wang et al., 2020), possibly explaining this result. Conversely, blocking CB_1 and 5-HT_{2A} receptors has prevented the increase in the threshold for the acute thermal pain stimulus. Our results align with previous studies on the SCRA **WIN55,212–2** showing that thermal antinociception after systemic administration is blocked by **ketanserin** (a 5-HT_2 receptor antagonist) and **risperidone** (an antagonist of 5-HT_{2A} and **5-HT_7** receptors) (Seyrek et al., 2010). Ultimately, this evidence suggests that AB-5′F-BUTINACA influences the nociceptive response in mice by acting on pathways different from those involved in reacting to mechanical (Martin et al., 1996) and thermal (Hohmann et al., 1999) pain stimuli.

The dose tested in the antagonistic study did not alter the rectal temperature of mice and the occurrence of major neurological changes prevented an increase in the dose. While the CB_1 antagonist NESS0327 had no influence on the rectal temperature, pretreatment with the 5-HT_{2A} antagonist MDL100907 induced a significant hypothermic effect. Previous studies revealed that indole-based SCRAs (e.g., AM-2201 and JWH-018) can potentiate hypothermia, typically mediated by **5-HT_{1A} receptors** in rodents (Elmore & Baumann, 2018; Yano et al., 2020). This indicates the involvement of other 5-HT receptor subtypes in the mechanisms underlying temperature homeostasis. Accordingly, a study investigating the complex interplay between 5-HT_{2A} and 5-HT_{1A} receptors demonstrated that the blockade of 5-HT_{1A} receptors can enhance 5-HT_{2A}-mediated behavioural effects (Glatfelter et al., 2024). In contrast, the hypothermic effect provoked by exposure to SCRAs (JWH-018 and 5F-PB-22) was prevented by the prior injection of MDL100907 (Corli, Tirri, et al., 2024). Therefore, the possibility that the highest dose of AB-5′F-BUTINACA-induced hypothermia could be prevented by pretreatment with the 5-HT_{2A} antagonist cannot be ruled out.

The respiratory patterns of mice were affected by AB-5′F-BUTINACA and were not prevented by pretreatment with NESS0327 or MDL100907. These results contradict previous research showing reduction in breathing rate evoked by SCRAs relies on CB_1 receptor activation in central (Pfitzer et al., 2004) and peripheral (Calignano et al., 2000) circuitries in rodents (Corli, Tirri, et al., 2024). Therefore, these results need further investigation as the lack of antagonism by the CB_1 antagonist NESS0327 may be explained by experimental factors, for example, dose of the antagonist, pharmacokinetics of the agonist and antagonist or observation times. Indeed, this study did not address the pharmacokinetic profile of these compounds, which is still to be elucidated. This may limit the ability to evaluate the influence of metabolites potentially retaining activity on CB_1 and 5-HT_{2A} receptors, thereby affecting its pharmaco-toxicological profile. Moreover, our results raise questions about the involvement of other receptor subtypes in the mechanisms underlying the compounds' specific pharmaco-toxicological effects (e.g., hypothermia and bradypnea).

On the other hand, the reduction in stepping activity was prevented by pretreatment with NESS0327 but not MDL100907, indicating that CB_1 receptor-mediated mechanisms primarily underlie the motor effects. This is in agreement with a previous study on indole-based SCRAs (Corli, Tirri, et al., 2024). Interestingly, injection of MDL100907 enhanced the hypo-locomotion induced by AB-5′F-BUTINACA. This is in line with a study demonstrating that the decreased locomotor activity caused by **m-chlorophenylpiperazine (mCPP)** is reduced by chronic administration of selective serotonin reuptake inhibitors (SSRIs) (Yamauchi et al., 2006).

This study demonstrated that the responses to AB-5′F-BUTINACA in vivo, including neurological, sensorimotor, and thermal antinociceptive effects, are mediated by CB_1 and 5-HT_{2A} receptors, as demonstrated by the selective antagonism experiments at CB_1 and 5-HT_{2A} receptors. However, as the endocannabinoid system has been found to modulate the serotonergic systems (Fantegrossi et al., 2018; Ibarra-Lecue et al., 2018, 2021; Ossato et al., 2017), it is not possible to conclude if these effects are a result of the compound's direct interaction with the 5-HT_{2A} receptor or if they result from an indirect interplay between the endocannabinoid and serotonergic systems. In addition, while the 5-HT_{2A} receptor is the primary target of psychedelic compounds, other 5-HT receptors, such as 5-HT_{1A}, **5-HT_{2B}**, and **5-HT_{2C}** receptors) may modulate their effects (Jain et al., 2025; Luethi et al., 2025). For example, the co-localization of CB_1 with either 5-HT_{1B} or **5-HT_3** receptors highlights potential cross-talk between the cannabinoid and serotonin neurotransmitter systems (Hermann et al., 2002). Therefore, 5-$HT_{1A/B}$, 5-HT_{2B}, and **5-HT_3** receptors warrant further investigation as modulators of cannabinoid signalling. Further, the results obtained in this study confirm the effectiveness of the Safety Pharmacology battery of tests in clarifying the pharmaco-toxicological profile (including behavioural, neurological and physiological responses) of emerging structurally diverse SCRAs and reducing the number of animals used (Canazza et al., 2016; Corli, Tirri, et al., 2024; Vigolo et al., 2015). Thus, this experimental protocol could be used in future studies aimed at investigating the pharmaco-toxicological profile of different valinamide (AB) or *tert*-leucinamide (ADB) cannabinoids.

5 | CONCLUSION

In conclusion, this study investigated the in vitro activity of various structurally diverse SCRAs at 5-HT_{2A} receptors, showing its activation by some valinamide- and *tert*-leucinamide-containing SCRAs, of which AB-5′F-BUTINACA and ADB-BUTINACA exhibited the highest efficacy. The in vivo evaluation of AB-5′F-BUTINACA found notable neurological changes, as well as sensorimotor, physiological (hypothermia and bradypnea), nociceptive and motor disruptions in mice, which

14765381, 2026, 16, Downloaded from https://bpspubs.onlinelibrary.wiley.com/doi/10.1111/bph.70457 by Universita Di Ferrara, Wiley Online Library on [20/10/2026]. See the Terms and Conditions (https://onlinelibrary.wiley.com/terms-and-conditions) on Wiley Online Library for rules of use; OA articles are governed by the applicable Creative Commons License

were prevented by pretreatment with selective CB_1 and 5-HT_{2A} receptor antagonists. However, the responses observed in this study raised further questions on the role of an interplay between the endocannabinoid and 5-HT neurotransmission systems and does not clarify the nature of antagonism. Further studies will be performed testing different doses of AB-5′F-BUTINACA in the presence of NESS0327 and M100907. These findings suggest that the 5-HT_{2A} receptors may be involved in the mechanisms underlying some of the acute effects of SCRAs in humans. Although it remains unclear whether the effects result mostly from the direct interaction with the 5-HT_{2A} receptor or CB_1 receptor mediation of the 5-HT system, from a translational point of view, this study adds to the understanding of risks associated with SCRA consumption, particularly the potential exacerbation of psychiatric symptoms mediated via 5-HT receptors.

ABBREVIATIONS

Δ^9-THC	Δ^9-tetrahydrocannabinol
3,5-ADB-4en-PFUPPYCA	(S)-N-(1-amino-3,3-dimethyl-1-oxobutan-2-yl)-3-(4-fluorophenyl)-1-(pent-4-en-1-yl)-1H-pyrazole-5-carboxamide; 3,5-4en-ADB-FUPPYCA
3OH-ADB-PropINACA	N-[(1S)-1-(aminocarbonyl)-2,2-dimethylpropyl]-1-(3-hydroxypropyl)-1H-indazole-3-carboxamide
4CN-Cumyl-BUT7AICA	1-(4-cyanobutyl)-N-(1-methyl-1-phenylethyl)-1H-pyrrolo[2,3-b]pyridine-3-carboxamide; 4CN-Cumyl-B7AICA; Cumy-4CN-B7AICA; 4-cyano Cumyl-BUT7AICA
5Cl-AB-PINACA	N-[(1S)-1-(aminocarbonyl)-2-methylpropyl]-1-(5-chloropentyl)-1H-indazole-3-carboxamide; 5-chloro ABP
5F-Cumyl-Pegaclone	5-(5-fluoropentyl)-2,5-dihydro-2-(1-methyl-1-phenylethyl)-1H-pyrido[4,3-b]indol-1-one; 5-fluoro SGT-151
5F-MDMB-PINACA	methyl 2-{[1-(5-fluoropentyl)-1H-indazole-3-carbonyl]amino}- 3,3-dimethylbutanoate; 5F-ADB
5F-PB-22	1-(5-fluoropentyl)-1H-Indole-3-carboxylic acid, 8-quinolinyl ester; 5F-QUPIC
AB	valinamide cannabinoid
(R)-AB-4en-PICA	N-[(1R)-1-(aminocarbonyl)-2-methyl propyl]-1-(4-penten-1-yl)-1H-indole-3-carboxamide; (R)-AMB-4en-PICA
AB-4en-PINACA	N-[(1S)-1-(aminocarbonyl)-2-methyl propyl]-1-(4-penten-1-yl)-1H-indazole-3-carboxamide; AMB-4en-PINACA
AB-5′Br-BUTINACA	N-[(1S)-1-(aminocarbonyl)-2-methylpropyl]-5-bromo-1-butyl-1H-indazole-3-carboxamide
AB-5′Cl-BUTINACA	N-[(1S)-1-(aminocarbonyl)-2-methylpropyl]-5-chloro-1-butyl-1H-indazole-3-carboxamide
AB-5′F-BUTINACA	N-[(1S)-1-(aminocarbonyl)-2-methylpropyl]-5-fluoro-1-butyl-1H-indazole-3-carboxamide
AB-CHMINACA	N-[(1S)-1-(aminocarbonyl)-2-methylpropyl]-1-(cyclohexylmethyl)-1H-indazole-3-carboxamide
AB-FUBINACA	N-[(1S)-1-(aminocarbonyl)-2-methylpropyl]-1-[(4-fluorophenyl)methyl]-1H-indazole-3-carboxamide
AB-HEXINACA	(S)-N-[(1S)-1-(aminocarbonyl)-2-methylpropyl]-1-hexyl-1H-indazole-3-carboxamide; AB-HINACA
AB-PINACA	N-[(1S)-1-(aminocarbonyl)-2-methylpropyl]-1-pentyl-1H-indazole-3-carboxamide
ACHMINACA	1-(cyclohexylmethyl)-N-tricyclo[3.3.1.1^{3,7}]dec-1-yl-1H-indazole-3-carboxamide
ADB	*tert*-leucinamide cannabinoid
ADB-4en-5′Br-PINACA	N-(1-amino-3,3-dimetyl-1-oxobutan-2-yl)-5-bromo-1-(pent-4-en-1-yl)-1H-indazol-3-karboxamid; ADMB-4en-5′Br-PINACA
ADB-4en-PICA	N-[1-(aminocarbonyl)-2,2-dimethylpropyl]-1-(4-penten-1-yl)-1H-indole-3-carboxamide
ADB-4en-PINACA	N-[1-(aminocarbonyl)-2,2-dimethylpropyl]-1-(4-penten-1-yl)-1H-indazole-3-carboxamide
ADB-5′Br-BUTINACA	(S)-N-(1-amino-3,3-dimethyl-1-oxobutan-2-yl)-5-bromo-1-butyl-1H-indazole-3-carboxamide; ADB-5′Br-BINACA; ADB-BUT-5Br-INACA
ADB-5′Br-DECINACA	(R)-N-(1-amino-3,3-dimethyl-1-oxobutan-2-yl)-5-bromo-1-decyl-1H-indazole-3-carboxamide; ADB-5′Br-DINACA; ADB-D-5Br-INACA
ADB-5′Cl-BUTINACA	(S)-N-(1-amino-3,3-dimethyl-1-oxobutan-2-yl)-5-chloro-1-butyl-1H-indazole-3-carboxamide
ADB-5′F-BUTINACA	(S)-N-(1-amino-3,3-dimethyl-1-oxobutan-2-yl)-5-fluoro-1-butyl-1H-indazole-3-carboxamide; ADB-B-5′F-INACA; ADB-BUT-5′F-INACA
ADB-5′Br-FUBINACA	N-[1-(aminocarbonyl)-2,2-dimethylpropyl]-1-[(4-fluorophenyl)methyl]-5-bromo-1H-indazole-3-carboxamide
ADB-5′Br-INACA	(S)-N-(1-Amino-3,3-dimethyl-1-oxobutan-2-yl)-5-bromo-1H-indazole-3-carboxamide
ADB-5′Br-PINACA	(S)-N-(1-amino-3,3-dimethyl-1-oxobutan-2-yl)-5-bromo-1-pentyl-1H-indazole-3-carboxamide; ADB-P-5′Br-INACA
ADB-BUTINACA	N-[(1S)-1-(aminocarbonyl)-2,2-dimethylpropyl]-1-butyl-1H-indazole-3-carboxamide
ADB-FUBIATA	N-[(1S)-1-(aminocarbonyl)-2,2-dimethylpropyl]-1-[(4-fluorophenyl)methyl]-1H-indole-3-acetamide
ADB-HEXICA	(S)-N-(1-amino-3,3-dimethyl-1-oxobutan-2-yl)-1-hexyl-1H-indole-3-carboxamide

14765381, 2026, 16, Downloaded from https://bpspubs.onlinelibrary.wiley.com/doi/10.1111/bph.70457 by Universita Di Ferrara, Wiley Online Library on [20/10/2026]. See the Terms and Conditions (https://onlinelibrary.wiley.com/terms-and-conditions) on Wiley Online Library for rules of use; OA articles are governed by the applicable Creative Commons License

ADB-HEXINACA	(S)-N-(1-amino-3,3-dimethyl-1-oxobutan-2-yl)-1-hexyl-1H-indazole-3-carboxamide; ADB-HINACA
ADB-ICA	N-[(1S)-1-(aminocarbonyl)-2,2-dimethylpropyl]-1H-indole-3-carboxamide
ADB-INACA	N-[(1S)-1-(aminocarbonyl)-2,2-dimethylpropyl]-1H-indazole-3-carboxamide
ADB-PINACA	N-[1-(aminocarbonyl)-2,2-dimethylpropyl]-1-pentyl-1H-indazole-3-carboxamide
ADB-PropINACA	N-[(1S)-1-(aminocarbonyl)-2,2-dimethylpropyl]-1-propyl-1H-indazole-3-carboxamide; ADB-Propyl-INACA
AM-2201	[1-(5-fluoropentyl)-1H-indol-3-yl]-1-naphthalenyl-methanone
ATP	adenosine-50-triphosphate disodium salt hydrate
AUC	area under the curve
BZO-HEXOXIZID	(2Z)-2-(1-hexyl-1,2-dihydro-2-oxo-3H-indol-3-ylidene)hydrazide, benzoic acid; MDA-19
CHO	Chinese hamster ovary
CHO-4′Me-5′Br-FUBOXPYRA	N-[5-bromo-1-[(4-fluorophenyl)methyl]-1,2-dihydro-4-methyl-2-oxo-3-pyridinyl]-cyclohexanecarboxamide; CH-FUBBMPDORA; 6TP
EMB-4en-PICA	ethyl 2-[[1-(pent-4-en-1-yl)indole-3-carbonyl]amino]-3-methylbutanoate
FLIPR	fluorescence imaging plate reader
HTRF	homogenous time-resolved fluorescence
IP_1	inositol monophosphate
JWH-018	1-naphthalenyl(1-pentyl-1H-indol-3-yl)-methanone
LSD	lysergic acid diethylamide
mCPP	m-chlorophenylpiperazine
MDL100907	(*R*)-(+)-α-(2,3-Dimethoxyphenyl)-1-[2-(4-fluorophenyl)ethyl]-4-piperinemethanol; Volinanserin
MDMB-5′F-BUTINACA	methyl (S)-2-(5-fluoro-1-butyl-1H-indazole-3-carboxamido)-3,3-dimethylbutanoate
MDMB-INACA	Methyl (S)-2-(1H-indazole-3-carboxamido)-3,3-dimethylbutanoate
MMB-5′F-BUTINACA	methyl (5-bromo-1-butyl-1H-indazole-3-carbonyl)-L-valinate
NESS0327	8-Chloro-1-(2,4-dichlorophenyl)-1,4,5,6-tetrahydro-*N*-1-piperidinyl-benzo[6,7]cyclohepta[1,2-*c*]pyrazole-3-carboxamide
NPS	new psychoactive substance
PB-22	1-pentyl-1H-indole-3-carboxylic acid, 8-quinolinyl ester; QUPIC
PFC	prefrontal cortex
PLC	phospholipase C
SARs	structure–activity relationships
SCRA	Synthetic cannabinoid receptor agonist
SSRIs	selective serotonin reuptake inhibitors

AUTHOR CONTRIBUTIONS

Giorgia Corli: Methodology; investigation; formal analysis; writing—original draft; visualization; writing—review and editing. **Deborah Rudin:** Methodology; investigation; writing—review and editing. **Dino Luethi:** Methodology; investigation; writing—review and editing. **Matthias Liechti E:** Supervision; writing—review and editing. **Sabrine Bilel:** Writing—review and editing. **Matteo Marti:** Supervision; writing—review and editing; funding acquisition. **Henrik Green:** Supervision; writing—review and editing; funding acquisition. **Manuela Carla Monti:** Conceptualization; methodology; investigation; formal analysis; writing—original draft; visualization; writing—review and editing; funding acquisition. **Caitlyn Norman:** Conceptualization; methodology; investigation; formal analysis; writing—original draft; visualization; writing—review and editing; funding acquisition.

ACKNOWLEDGEMENTS

The authors thank Urs Duthaler from the Institute of Forensic Medicine Basel and Christian Bissig from the Zurich Forensic Science Institute for coordination and provision of some reference standards to the University of Basel. The Swedish-led aspects of the study received funding from the Eurostars-3 Joint Programme (European Commission, E!2297 [Eurostars-3], EUFORiaR, European Union Forensic Intelligence and Reference Materials, a collaboration between LiU and Chiron AS) with co-funding from the European Union's Horizon 2020 research and innovation programme, VINNOVA (Sweden's Innovation Agency; Grant Number 2019-03566) and the Swiss National Science Foundation (SNSF) within the Postdoc. Mobility funding scheme (Grant Number 217677 for M. C. M.), Svenska Sällskapet för Medicinsk Forskning (Swedish Society for Medical Research, SSMF; Postdoctoral Grant 2024, PG-24-0356-H-01 for C. N.) and the Strategic Research Area in Forensic Sciences (Strategiområdet forensiska vetenskaper) at Linköping University. The in vivo aspects of the study were funded by the Anti-Drug Policies Department, Presidency of the Council of Ministers, Italy (project: 'Multicenter research for the Study of the pharmaco-toxicological effects and analytical identification of new synthetic opioids and NPS' to M. M.) and local funds from the University of Ferrara (FAR 2024, FAR 2025 to M. M.).

CONFLICT OF INTEREST STATEMENT

M.E.L. is a consultant for Lykos Therapeutics. The other authors do not report any conflicts of interest.

DATA AVAILABILITY STATEMENT

The data that support the findings of this study are available from the corresponding author upon reasonable request. Some data may not be made available because of privacy or ethical restrictions.

DECLARATION OF TRANSPARENCY AND SCIENTIFIC RIGOUR

This declaration acknowledges that this paper adheres to the principles for transparent reporting and scientific rigour of preclinical research as stated in the *BJP* guidelines for Design and Analysis and

14765381, 2026, 16, Downloaded from https://bpspubs.onlinelibrary.wiley.com/doi/10.1111/bph.70457 by Universita Di Ferrara, Wiley Online Library on [20/10/2026]. See the Terms and Conditions (https://onlinelibrary.wiley.com/terms-and-conditions) on Wiley Online Library for rules of use; OA articles are governed by the applicable Creative Commons License

Animal Experimentation, and as recommended by funding agencies, publishers and other organisations engaged with supporting research.

ORCID

Giorgia Corli https://orcid.org/0000-0002-2973-2446
Deborah Rudin https://orcid.org/0000-0003-3069-9732
Dino Luethi https://orcid.org/0000-0003-0874-4875
Matthias E. Liechti https://orcid.org/0000-0002-1765-9659
Sabrine Bilel https://orcid.org/0000-0003-1515-980X
Matteo Marti https://orcid.org/0000-0001-8751-2882
Henrik Green https://orcid.org/0000-0002-8015-5728
Manuela Carla Monti https://orcid.org/0000-0002-9959-398X
Caitlyn Norman https://orcid.org/0000-0003-2322-0367

REFERENCES

Abouchedid, R., Hudson, S., Thurtle, N., Yamamoto, T., Ho, J. H., Bailey, G., Wood, M., Sadones, N., Stove, C. P., Dines, A., Archer, J. R. H., Wood, D. M., & Dargan, P. I. (2017). Analytical confirmation of synthetic cannabinoids in a cohort of 179 presentations with acute recreational drug toxicity to an Emergency Department in London, UK in the first half of 2015. *Clinical Toxicology*, *55*(5), 338–345. https://doi.org/10.1080/15563650.2017.1287373

Alexander, S. P. H., Davenport, A. P., Kelly, E., Gibb, A. J., Mathie, A. A., Peach, C. J., Veale, E. L., Armstrong, J. F., Faccenda, E., Harding, S. D., Southan, C., Davies, J. A., Abbracchio, M. P., Abraham, G. R., Agoulnik, A., Alexander, W., Al-hosaini, K., Bäck, M., Baker, J. G., … Zaidman, N. (2025). The concise guide to pharmacology 2025/26: G protein-coupled receptors. *British Journal of Pharmacology*, *182*(S1), S24–S151. https://doi.org/10.1111/bph.70230

Alexander, S. P. H., Striessnig, J., Gibb, A. J., Mathie, A. A., Veale, E. L., Kelly, E., Peach, C. J., Armstrong, J. F., Faccenda, E., Harding, S. D., Southan, C., Davies, J. A., Aldrich, R. W., Attali, B., Baggetta, A. M., Becirovic, E., Beech, D. J., Biel, M., Bill, R. M., … Zhu, M. (2025). The Concise Guide to PHARMACOLOGY 2025/26: Ion channels. *British Journal of Pharmacology*, *182*(Suppl 1), S152–S241. https://doi.org/10.1111/bph.70231

Amodeo, D. A., Rivera, E., Cook, E. H., Sweeney, J. A., & Ragozzino, M. E. (2017). 5HT2A receptor blockade in dorsomedial striatum reduces repetitive behaviors in BTBR mice. *Genes, Brain, and Behavior*, *16*(3), 342–351. https://doi.org/10.1111/gbb.12343

Arfè, R., Bilel, S., Tirri, M., Frisoni, P., Serpelloni, G., Neri, M., Boccuto, F., Bernardi, T., Foti, F., De-Giorgio, F., & Marti, M. (2021). Comparison of N-methyl-2-pyrrolidone (NMP) and the "date rape" drug GHB: behavioral toxicology in the mouse model. *Psychopharmacology*, *238*(8), 2275–2295. https://doi.org/10.1007/s00213-021-05852-5

Arias, H. R., Rudin, D., Hines, D. J., Contreras, A., Gulsevin, A., Manetti, D., Anouar, Y., De Deurwaerdere, P., Meiler, J., Romanelli, M. N., Liechti, M. E., & Chagraoui, A. (2024). The novel non-hallucinogenic compound DM506 (3-methyl-1,2,3,4,5,6-hexahydroazepino[4,5-b]indole) induces sedative- and anxiolytic-like activity in mice by a mechanism involving 5-HT2A receptor activation. *European Journal of Pharmacology*, *966*, 176329. https://doi.org/10.1016/j.ejphar.2024.176329

Åstrand, A., Guerrieri, D., Vikingsson, S., Kronstrand, R., & Green, H. (2020). In vitro characterization of new psychoactive substances at the μ-opioid, CB1, 5HT1A, and 5-HT2A receptors—On-target receptor potency and efficacy, and off-target effects. *Forensic Science International*, *317*, 110553. https://doi.org/10.1016/j.forsciint.2020.110553

Baginski, S. R., Rautio, T., Nisbet, L. A., Lindbom, K., Wu, X., Dahlen, J., McKenzie, C., & Green, H. (2023). The metabolic profile of the synthetic cannabinoid receptor agonist ADB-HEXINACA using human hepatocytes, LC–QTOF-MS and synthesized reference standards. *Journal of Analytical Toxicology*, *47*(9), 826–834. https://doi.org/10.1093/jat/bkad065

Bilel, S., Tirri, M., Arfè, R., Ossato, A., Trapella, C., Serpelloni, G., Neri, M., Fattore, L., & Marti, M. (2020). Novel halogenated synthetic cannabinoids impair sensorimotor functions in mice. *Neurotoxicology*, *76*, 17–32. https://doi.org/10.1016/j.neuro.2019.10.002

Bilel, S., Zamberletti, E., Caffino, L., Tirri, M., Mottarlini, F., Arfè, R., Barbieri, M., Beggiato, S., Boccuto, F., Bernardi, T., Casati, S., Brini, A. T., Parolaro, D., Rubino, T., Ferraro, L., Fumagalli, F., & Marti, M. (2023). Cognitive dysfunction and impaired neuroplasticity following repeated exposure to the synthetic cannabinoid JWH-018 in male mice. *British Journal of Pharmacology*, *180*(21), 2777–2801. https://doi.org/10.1111/bph.16164

Bush, D. M., & Woodwell, D. A. (2014). Update: Drug-Related Emergency Department Visits Involving Synthetic Cannabinoids. In The CBHS Report is a book published by Substance Abuse and Mental Health Services Administration in Rockville, MD.

Calignano, A., Kátona, I., Désarnaud, F., Giuffrida, A., La Rana, G., Mackie, K., Freund, T. F., & Piomelli, D. (2000). Bidirectional control of airway responsiveness by endogenous cannabinoids. *Nature*, *408*(6808), 96–101. https://doi.org/10.1038/35040576

Campos-Ordoñez, T., Alcalá, E., Ibarra-Castañeda, N., Buriticá, J., & González-Pérez, Ó. (2022). Chronic exposure to cyclohexane induces stereotypic circling, hyperlocomotion, and anxiety-like behavior associated with atypical c-Fos expression in motor- and anxiety-related brain regions. *Behavioural Brain Research*, *418*, 113664. https://doi.org/10.1016/j.bbr.2021.113664

Canazza, I., Ossato, A., Trapella, C., Fantinati, A., De Luca, M. A., Margiani, G., Vincenzi, F., Rimondo, C., Di Rosa, F., Gregori, A., Varani, K., Borea, P. A., Serpelloni, G., & Marti, M. (2016). Effect of the novel synthetic cannabinoids AKB48 and 5F-AKB48 on "tetrad", sensorimotor, neurological and neurochemical responses in mice. In vitro and in vivo pharmacological studies. *Psychopharmacology*, *233*, 3685–3709. https://doi.org/10.1007/s00213-016-4402-y

Castellanos, D., Singh, S., Thornton, G., Avila, M., & Moreno, A. (2011). Synthetic cannabinoid use: A case series of adolescents. *Journal of Adolescent Health*, *49*(4), 347–349. https://doi.org/10.1016/j.jadohealth.2011.08.002

Chambers, J. J., & Nichols, D. E. (2002). A homology-based model of the human 5-HT2A receptor derived from an in silico activated G-protein coupled receptor. *Journal of Computer-Aided Molecular Design*, *16*(7), 511–520. https://doi.org/10.1023/A:1021275430021

Corli, G., Roda, E., Tirri, M., Bilel, S., De Luca, F., Strano-Rossi, S., Gaudio, R. M., De-Giorgio, F., Fattore, L., Locatelli, C. A., & Marti, M. (2024). Sex-specific behavioural, metabolic, and immunohistochemical changes after repeated administration of the synthetic cannabinoid AKB48 in mice. *British Journal of Pharmacology*, *181*(9), 1361–1382. https://doi.org/10.1111/bph.16311

Corli, G., Tirri, M., Arfè, R., Bilel, S., Marchetti, B., Gregori, A., Di Rosa, F., Vincenzi, F., De-Giorgio, F., Borea, P. A., Varani, K., & Marti, M. (2022). Behavioral and binding studies on the quinolinyl ester indoles 5F-PB22 (5F-QUPIC) and BB-22 (QUCHIC) in the mouse model. *Emerging Trends in Drugs, Addictions, and Health*, *2*, 100039. https://doi.org/10.1016/j.etdah.2022.100039

Corli, G., Tirri, M., Bassi, M., Bernardi, T., Boccuto, F., Borsari, M., Zauli, G., Bilel, S., & Marti, M. (2024). 5-HT2A receptors are involved in the pharmaco-toxicological effects of the synthetic cannabinoids JWH-018 and 5F-PB22: In vivo studies in mice. *European Journal of Pharmacology*, *971*, 176486. https://doi.org/10.1016/j.ejphar.2024.176486

Darke, S., Banister, S., Farrell, M., Duflou, J., & Lappin, J. (2021). Synthetic cannabis': A dangerous misnomer. *International Journal of Drug Policy*, *98*, 103396. https://doi.org/10.1016/j.drugpo.2021.103396

Deng, L., Vysotski, E. S., Markova, S. V., Liu, Z.-J., Lee, J., Rose, J., & Wang, B.-C. (2009). All three Ca2+−binding loops of photoproteins

14765381, 2026, 16, Downloaded from https://bpspubs.onlinelibrary.wiley.com/doi/10.1111/bph.70457 by Universita Di Ferrara, Wiley Online Library on [20/10/2026]. See the Terms and Conditions (https://onlinelibrary.wiley.com/terms-and-conditions) on Wiley Online Library for rules of use; OA articles are governed by the applicable Creative Commons License

bind calcium ions: The crystal structures of calcium-loaded apo-aequorin and apo-obelin. *Protein Science*, *14*(3), 663–675. https://doi.org/10.1110/ps.041142905

Elmore, J. S., & Baumann, M. H. (2018). Repeated exposure to the "spice" cannabinoid JWH-018 induces tolerance and enhances responsiveness to 5-HT1A receptor stimulation in male rats. *Frontiers in Psychiatry*, *9*, 1–8. https://doi.org/10.3389/fpsyt.2018.00055

Fantegrossi, W. E., Wilson, C. D., & Berquist, M. D. (2018). Pro-psychotic effects of synthetic cannabinoids: interactions with central dopamine, serotonin, and glutamate systems. *Drug Metabolism Reviews*, *50*(1), 65–73. https://doi.org/10.1080/03602532.2018.1428343

Glatfelter, G. C., Clark, A. A., Cavalco, N. G., Landavazo, A., Partilla, J. S., Naeem, M., Golen, J. A., Chadeayne, A. R., Manke, D. R., Blough, B. E., McCorvy, J. D., & Baumann, M. H. (2024). Serotonin 1A Receptors Modulate Serotonin 2A Receptor-Mediated Behavioral Effects of 5-Methoxy-N,N-dimethyltryptamine Analogs in Mice. *ACS Chemical Neuroscience*, *15*(24), 4458–4477. https://doi.org/10.1021/acschemneuro.4c00513

Grafinger, K. E., Cannaert, A., Ametovski, A., Sparkes, E., Cairns, E., Banister, S. D., Auwärter, V., & Stove, C. P. (2021). Systematic evaluation of a panel of 30 synthetic cannabinoid receptor agonists structurally related to MMB-4en-PICA, MDMB-4en-PINACA, ADB-4en-PINACA, and MMB-4CN-BUTINACA using a combination of binding and different CB1receptor activation assays—part II: structure activity relationship assessment via a β-arrestin recruitment assay. *Drug Testing and Analysis*, *13*(7), 1402–1411. https://doi.org/10.1002/dta.3035

Green, H., McKenzie, C., Hamra, E., Rautio, T., Wu, X., Juneskog, E., Sandblom, R., Monti, M. C., Persson, M., & Norman, C. (2025). In vitro CB1 receptor activity of halogenated indazole synthetic cannabinoid receptor agonists. *Archives of Toxicology*, *99*, 3343–3353. https://doi.org/10.1007/s00204-025-04082-4

Haj-Dahmane, S., & Shen, R. Y. (2011). Modulation of the serotonin system by endocannabinoid signaling. *Neuropharmacology*, *61*(3), 414–420. https://doi.org/10.1016/j.neuropharm.2011.02.016

Hermann, H., Marsicano, G., & Lutz, B. (2002). Coexpression of the cannabinoid receptor type 1 with dopamine and serotonin receptors in distinct neuronal subpopulations of the adult mouse forebrain. *Neuroscience*, *109*(3), 451–460. https://doi.org/10.1016/S0306-4522(01)00509-7

Hill, M. N., Sun, J. C., Tse, M. T. L., & Gorzalka, B. B. (2006). Altered responsiveness of serotonin receptor subtypes following long-term cannabinoid treatment. *International Journal of Neuropsychopharmacology*, *9*(3), 277–286. https://doi.org/10.1017/S1461145705005651

Hohmann, A. G., Tsou, K., & Walker, J. M. (1999). Cannabinoid suppression of noxious heat-evoked activity in wide dynamic range neurons in the lumbar dorsal horn of the rat. *Journal of Neurophysiology*, *81*(2), 575–583. https://doi.org/10.1152/jn.1999.81.2.575

Ibarra-Lecue, I., Diez-Alarcia, R., & Urigüen, L. (2021). Serotonin 2A receptors and cannabinoids. In N. Moradikor, M. Haghipanah, & H. Hamdar (Eds.), *Progress in Brain Research* (Vol. 294, pp. 135–175). Elsevier. https://doi.org/10.1016/bs.pbr.2021.01.004

Ibarra-Lecue, I., Mollinedo-Gajate, I., Meana, J. J., Callado, L. F., Diez-Alarcia, R., & Urigüen, L. (2018). Chronic cannabis promotes pro-hallucinogenic signaling of 5-HT2A receptors through Akt/mTOR pathway. *Neuropsychopharmacology*, *43*(10), 2028–2035. https://doi.org/10.1038/s41386-018-0076-y

Jain, M. K., Gumpper, R. H., Slocum, S. T., Schmitz, G. P., Madsen, J. S., Tummino, T. A., Suomivuori, C.-M., Huang, X.-P., Shub, L., DiBerto, J. F., Kim, K., DeLeon, C., Krumm, B. E., Fay, J. F., Keiser, M., Hauser, A. S., Dror, R. O., Shoichet, B., Gloriam, D. E., … Roth, B. L. (2025). The polypharmacology of psychedelics reveals multiple targets for potential therapeutics. *Neuron*, *113*(19), 3129–3142.e9. https://doi.org/10.1016/j.neuron.2025.06.012

Kak, M., Mikhail, F., Yano, S. T., Guan, R., & Lukas, R. V. (2017). Buzz Juice: Neurological sequelae of synthetic cannabinoids. *Journal of Clinical Neuroscience*, *37*, 43. https://doi.org/10.1016/j.jocn.2016.10.046

Kehne, J., Baron, B., Carr, A., Chaney, S., Elands, J., Feldman, D., Frank, R., van Giersbergen, P., McCloskey, T., Johnson, M., McCarty, D., Poirot, M., Senyah, Y., Siegel, B., & Widmaier, C. (1996). Preclinical characterization of the potential of the putative atypical antipsychotic MDL 100,907 as a potent 5-HT2A antagonist with a favorable CNS safety profile. *Journal of Pharmacology and Experimental Therapeutics*, *277*(2), 968–981.

Kristiansen, K., Kroeze, W. K., Willins, D. L., Gelber, E. I., Savage, J. E., Glennon, R. A., & Roth, B. L. (2000). A Highly Conserved Aspartic Acid (Asp-155) Anchors the Terminal Amine Moiety of Tryptamines and Is Involved in Membrane Targeting of the 5-HT 2A Serotonin Receptor But Does Not Participate in Activation via a "Salt-Bridge Disruption" Mechanism 1. *The Journal of Pharmacology and Experimental Therapeutics*, *293*(3), 735–746. https://doi.org/10.1016/S0022-3565(24)39293-6

Kronstrand, R., Norman, C., Vikingsson, S., Biemans, A., Crespo, B. V., Edwards, D., Fletcher, D., Gilbert, N., Persson, M., Reid, R., Semenova, O., Al Teneiji, F., Wu, X., Dahlén, J., Nic Daéid, N., Tarbah, F., Sutcliffe, O. B., McKenzie, C., & Gréen, H. (2022). The metabolism of the synthetic cannabinoids ADB-BUTINACA and ADB-4en-PINACA and their detection in forensic toxicology casework and infused papers seized in prisons. *Drug Testing and Analysis*, *14*(4), 634–652. https://doi.org/10.1002/dta.3203

Lilley, E., Stanford, S. C., Kendall, D. E., Alexander, S. P. H., Cirino, G., Docherty, J. R., George, C. H., Insel, P. A., Izzo, A. A., Ji, Y., Panettieri, R. A., Sobey, C. G., Stefanska, B., Stephens, G., Teixeira, M., & Ahluwalia, A. (2020). ARRIVE 2.0 and the British Journal of Pharmacology: Updated guidance for 2020. *British Journal of Pharmacology*, *177*(16), 3611–3616. https://doi.org/10.1111/bph.15178

Lin, F., Li, F., Wang, C., Wang, J., Yang, Y., Yang, L., & Li, Y. (2017). Mechanism exploration of arylpiperazine derivatives targeting the 5-HT2A receptor by in silico methods. *Molecules*, *22*(7), 1–22. https://doi.org/10.3390/molecules22071064

Lin, S., Lee, L., & Yang, Y. K. (2014). Serotonin and mental disorders: A concise review on molecular neuroimaging evidence. *Clinical Psychopharmacology and Neuroscience*, *12*(3), 196–202. https://doi.org/10.9758/cpn.2014.12.3.196

Luethi, D., Glatfelter, G. C., Pottie, E., Sellitti, F., Maitland, A. D., Gonzalez, N. R., Kryszak, L. A., Jackson, S. N., Hoener, M. C., Stove, C. P., Liechti, M. E., Smieško, M., Baumann, M. H., Simmler, L. D., & Rudin, D. (2025). The 4-alkyl chain length of 2,5-dimethoxyamphetamines differentially affects in vitro serotonin receptor actions versus in vivo psychedelic-like effects. *Molecular Psychiatry*, *31*, 1799–1809. https://doi.org/10.1038/s41380-025-03325-1

Martin, W. J., Hohmann, A. G., & Walker, J. M. (1996). Suppression of noxious stimulus-evoked activity in the ventral posterolateral nucleus of the thalamus by a cannabinoid agonist: Correlation between electrophysiological and antinociceptive effects. *Journal of Neuroscience*, *16*(20), 6601–6611. https://doi.org/10.1523/jneurosci.16-20-06601.1996

Mason, G. (1991). Stereotypies: a critical review. *Animal Behaviour*, *41*(6), 1015–1037. https://doi.org/10.1016/S0003-3472(05)80640-2

Metna-Laurent, M., Mondesir, M., Grel, A., Vallee, M., & Piazza, P.-V. (2018). Cannabinoid-induced tetrad in mice. *Current Protocols in Neuroscience*, *80*, 9–59. https://doi.org/10.1002/cpns.31

Monti, M. C., Rautio, T., Deventer, M. H., Schläpfer, M., Tveit, J., Krotulski, A. J., Marland, V., Reid, R., Daeid, N. N., McKenzie, C., Stove, C. P., Green, H., & Norman, C. (2025). Tail-less precursors in synthetic cannabinoid production: investigating a clandestine laboratory, seized samples, and CB1 activity. *Archives of Toxicology*, *99*, 3641–3661. https://doi.org/10.1007/s00204-025-04086-0

Moranta, D., Esteban, S., & Garcia-Sevilla, J. A. (2004). Differential effects of acute cannabinoid drug treatment, mediated by CB1 receptors, on the in vivo activity of tyrosine and tryptophan hydroxylase in the rat

14765381, 2026, 16, Downloaded from https://bpspubs.onlinelibrary.wiley.com/doi/10.1111/bph.70457 by Universita Di Ferrara, Wiley Online Library on [20/10/2026]. See the Terms and Conditions (https://onlinelibrary.wiley.com/terms-and-conditions) on Wiley Online Library for rules of use; OA articles are governed by the applicable Creative Commons License

brain. *Naunyn-Schmiedeberg's Archives of Pharmacology*, *369*, 516–524. https://doi.org/10.1007/s00210-004-0921-x

Nair, A. B., & Jacob, S. (2016). A simple practice guide for dose conversion between animals and human. *Journal of Basic and Clinical Pharmacy*, *7*(2), 27–31. https://doi.org/10.4103/0976-0105.177703

Nakazi, M., Bauer, U., Nickel, T., Kathmann, M., & Schlicker, E. (2000). Inhibition of serotonin release in the mouse brain via presynaptic cannabinoid CB 1 receptors. *Naunyn-Schmiedeberg's Archives of Pharmacology*, *361*, 19–24. https://doi.org/10.1007/s002109900147

Nichols, D. E. (2012). Structure-activity relationships of serotonin 5-HT2A agonists. *Wiley Interdisciplinary Reviews: Membrane Transport and Signaling*, *1*(5), 559–579. https://doi.org/10.1002/wmts.42

Noble, C., Cannaert, A., Linnet, K., & Stove, C. P. (2019). Application of an activity-based receptor bioassay to investigate the in vitro activity of selected indole- and indazole-3-carboxamide-based synthetic cannabinoids at CB1 and CB2 receptors. *Drug Testing and Analysis*, *11*, 501–511. https://doi.org/10.1002/dta.2517

Ossato, A., Canazza, I., Trapella, C., Vincenzi, F., De Luca, M. A., Rimondo, C., Varani, K., Borea, P. A., Serpelloni, G., & Marti, M. (2016). Effect of JWH-250, JWH-073 and their interaction on "tetrad", sensorimotor, neurological and neurochemical responses in mice. *Progress in Neuro-Psychopharmacology and Biological Psychiatry*, *67*, 31–50. https://doi.org/10.1016/j.pnpbp.2016.01.007

Ossato, A., Uccelli, L., Bilel, S., Canazza, I., Di Domenico, G., Pasquali, M., Pupillo, G., De Luca, M. A., Boschi, A., Vincenzi, F., Rimondo, C., Beggiato, S., Ferraro, L., Varani, K., Borea, P. A., Serpelloni, G., DeGiorgio, F., & Marti, M. (2017). Psychostimulant effect of the synthetic cannabinoid JWH-018 and AKB48: Behavioral, neurochemical, and dopamine transporter scan imaging studies in mice. *Frontiers in Psychiatry*, *8*, 1–13. https://doi.org/10.3389/fpsyt.2017.00130

Percie du Sert, N., Hurst, V., Ahluwalia, A., Alam, S., Avey, M. T., Baker, M., Browne, W. J., Clark, A., Cuthill, I. C., Dirnagl, U., Emerson, M., Garner, P., Holgate, S. T., Howells, D. W., Karp, N. A., Lazic, S. E., Lidster, K., MacCallum, C. J., Macleod, M., … Würbel, H. (2020). The ARRIVE guidelines 2.0: Updated guidelines for reporting animal research. *British Journal of Pharmacology*, *177*(16), 3617–3624. https://doi.org/10.1111/bph.15193

Peters, K. Z., Cheer, J. F., & Tonini, R. (2021). Modulating the Neuromodulators: Dopamine, Serotonin, and the Endocannabinoid System. *Trends in Neurosciences*, *44*(6), 464–477. https://doi.org/10.1016/j.tins.2021.02.001

Pfitzer, T., Niederhoffer, N., & Szabo, B. (2004). Central effects of the cannabinoid receptor agonist WIN55212-2 on respiratory and cardiovascular regulation in anaesthetised rats. *British Journal of Pharmacology*, *142*(6), 943–952. https://doi.org/10.1038/sj.bjp.0705874

Rautio, T., Connolly, M., Liu, H., Konradsson, P., Gréen, H., Dahlén, J., & Wu, X. (2024). Direct and selective alkylation of indazole-3-carboxylic acid for the preparation of synthetic cannabinoids and their metabolites. *Forensic Chemistry*, *40*, 100603. https://doi.org/10.1016/j.forc.2024.100603

Rodriguiz, R. M., Nadkarni, V., Means, C. R., Pogorelov, V. M., Chiu, Y. T., Roth, B. L., & Wetsel, W. C. (2021). LSD-stimulated behaviors in mice require β-arrestin 2 but not β-arrestin 1. *Scientific Reports*, *11*(1), 1–14. https://doi.org/10.1038/s41598-021-96736-3

Salaga, M., Binienda, A., Piscitelli, F., Mokrowiecka, A., Cygankiewicz, A. I., Verde, R., Malecka-Panas, E., Kordek, R., Krajewska, W. M., Di Marzo, V., & Fichna, J. (2019). Systemic administration of serotonin exacerbates abdominal pain and colitis via interaction with the endocannabinoid system. *Biochemical Pharmacology*, *161*, 37–51. https://doi.org/10.1016/j.bcp.2019.01.001

Schep, L. J., Slaughter, R. J., Hudson, S., Place, R., & Watts, M. (2015). Delayed seizure-like activity following analytically confirmed use of previously unreported synthetic cannabinoid analogues. *Human and Experimental Toxicology*, *34*(5), 557–560. https://doi.org/10.1177/0960327114550886

Seyrek, M., Kahraman, S., Deveci, M. S., Yesilyurt, O., & Dogrul, A. (2010). Systemic cannabinoids produce CB1-mediated antinociception by activation of descending serotonergic pathways that act upon spinal 5-HT7 and 5-HT2A receptors. *European Journal of Pharmacology*, *649*(1–3), 183–194. https://doi.org/10.1016/j.ejphar.2010.09.039

Steffens, M., & Feuerstein, T. J. (2004). Receptor-independent depression of DA and 5-HT uptake by cannabinoids in rat neocortex - Involvement of Na+/K+-ATPase. *Neurochemistry International*, *44*(7), 529–538. https://doi.org/10.1016/j.neuint.2003.08.009

Vigolo, A., Ossato, A., Trapella, C., Vincenzi, F., Rimondo, C., Seri, C., Varani, K., Serpelloni, G., & Marti, M. (2015). Novel halogenated derivates of JWH-018: Behavioral and binding studies in mice. *Neuropharmacology*, *95*, 68–82. https://doi.org/10.1016/j.neuropharm.2015.02.008

Viñals, X., Moreno, E., Lanfumey, L., Cordomí, A., Pastor, A., De La Torre, R., Gasperini, P., Navarro, G., Howell, L. A., Pardo, L., Lluís, C., Canela, E. I., McCormick, P. J., Maldonado, R., & Robledo, P. (2015). Cognitive impairment induced by delta9-tetrahydrocannabinol occurs through heteromers between cannabinoid CB1 and serotonin 5-HT2A receptors. *PLoS Biology*, *13*(7), 1–40. https://doi.org/10.1371/journal.pbio.1002194

Wang, X. F., Galaj, E., Bi, G. H., Zhang, C., He, Y., Zhan, J., Bauman, M. H., Gardner, E. L., & Xi, Z. X. (2020). Different receptor mechanisms underlying phytocannabinoid- versus synthetic cannabinoid-induced tetrad effects: Opposite roles of CB1/CB2 versus GPR55 receptors. *British Journal of Pharmacology*, *177*(8), 1865–1880. https://doi.org/10.1111/bph.14958

Wiley, J. L., Lefever, T. W., Glass, M., & Thomas, B. F. (2019). Do you feel it now? Route of administration and Δ9-tetrahydrocannabinol-like discriminative stimulus effects of synthetic cannabinoids in mice. *Neurotoxicology*, *73*, 161–167. https://doi.org/10.1016/j.neuro.2019.04.002

Wiley, J. L., Lefever, T. W., Marusich, J. A., Grabenauer, M., Moore, K. N., Huffman, J. W., & Thomas, B. F. (2016). Evaluation of first generation synthetic cannabinoids on binding at non-cannabinoid receptors and in a battery of in vivo assays in mice. *Neuropharmacology*, *110*, 143–153. https://doi.org/10.1016/j.neuropharm.2016.07.016

Wouters, E., Walraed, J., Banister, S. D., & Stove, C. P. (2019). Insights into biased signaling at cannabinoid receptors: Synthetic cannabinoid receptor agonists. *Biochemical Pharmacology*, *169*, 113623. https://doi.org/10.1016/j.bcp.2019.08.025

Yamauchi, M., Miyara, T., Matsushima, T., & Imanishi, T. (2006). Desensitization of 5-HT2A receptor function by chronic administration of selective serotonin reuptake inhibitors. *Brain Research*, *1067*(1), 164–169. https://doi.org/10.1016/j.brainres.2005.10.075

Yano, H., Adhikari, P., Naing, S., Hoffman, A. F., Baumann, M. H., Lupica, C. R., & Shi, L. (2020). Positive Allosteric Modulation of the 5-HT1A Receptor by Indole-Based Synthetic Cannabinoids Abused by Humans. *ACS Chemical Neuroscience*, *11*(10), 1400–1405. https://doi.org/10.1021/acschemneuro.0c00034

SUPPORTING INFORMATION

Additional supporting information can be found online in the Supporting Information section at the end of this article.

How to cite this article: Corli, G., Rudin, D., Luethi, D., Liechti, M. E., Bilel, S., Marti, M., Green, H., Monti, M. C., & Norman, C. (2026). 5-HT_{2A} receptor agonism by *tert*-leucinamide and valinamide synthetic cannabinoids: In vitro and in vivo evidence. *British Journal of Pharmacology*, *183*(16), 4715–4734. https://doi.org/10.1111/bph.70457

14765381, 2026, 16, Downloaded from https://bpspubs.onlinelibrary.wiley.com/doi/10.1111/bph.70457 by Universita Di Ferrara, Wiley Online Library on [20/10/2026]. See the Terms and Conditions (https://onlinelibrary.wiley.com/terms-and-conditions) on Wiley Online Library for rules of use; OA articles are governed by the applicable Creative Commons License